Brain Advance Access published September 27, 2016

BRAIN
A JOURNAL OF NEUROLOGY

Your perspective and my benefit: multiple lesion models of self-other integration strategies during social bargaining

Margherita Melloni,[1,2,*] Pablo Billeke,[3,*] Sandra Baez,[1,2] Eugenia Hesse,[1,4] Laura de la Fuente,[1] Gonzalo Forno,[5,13], Agustina Birba,[1,2] Indira García-Cordero,[1] Cecilia Serrano,[6] Angelo Plastino,[2,7,8] Andrea Slachevsky,[5,9,10,11,12] David Huepe,[13] Mariano Sigman,[14,15] Facundo Manes,[1] Adolfo M. García,[1,2,16] Lucas Sedeño[1,2] and Agustín Ibáñez[1,2,13,17,18]

*These authors contributed equally to this work.

Recursive social decision-making requires the use of flexible, context-sensitive long-term strategies for negotiation. To succeed in social bargaining, participants' own perspectives must be dynamically integrated with those of interactors to maximize self-benefits and adapt to the other's preferences, respectively. This is a prerequisite to develop a successful long-term self-other integration strategy. While such form of strategic interaction is critical to social decision-making, little is known about its neurocognitive correlates. To bridge this gap, we analysed social bargaining behaviour in relation to its structural neural correlates, ongoing brain dynamics (oscillations and related source space), and functional connectivity signatures in healthy subjects and patients offering contrastive lesion models of neurodegeneration and focal stroke: behavioural variant frontotemporal dementia, Alzheimer's disease, and frontal lesions. All groups showed preserved basic bargaining indexes. However, impaired self-other integration strategy was found in patients with behavioural variant frontotemporal dementia and frontal lesions, suggesting that social bargaining critically depends on the integrity of prefrontal regions. Also, associations between behavioural performance and data from voxel-based morphometry and voxel-based lesion–symptom mapping revealed a critical role of prefrontal regions in value integration and strategic decisions for self-other integration strategy. Furthermore, as shown by measures of brain dynamics and related sources during the task, the self-other integration strategy was predicted by brain anticipatory activity (alpha/beta oscillations with sources in frontotemporal regions) associated with expectations about others' decisions. This pattern was reduced in all clinical groups, with greater impairments in behavioural variant frontotemporal dementia and frontal lesions than Alzheimer's disease. Finally, connectivity analysis from functional magnetic resonance imaging evidenced a fronto-temporo-parietal network involved in successful self-other integration strategy, with selective compromise of long-distance connections in frontal disorders. In sum, this work provides unprecedented evidence of convergent behavioural and neurocognitive signatures of strategic social bargaining in different lesion models. Our findings offer new insights into the critical roles of prefrontal hubs and associated temporo-parietal networks for strategic social negotiation.

1 Laboratory of Experimental Psychology and Neuroscience (LPEN), Institute of Cognitive and Translational Neuroscience (INCyT), INECO Foundation, Favaloro University, Buenos Aires, Argentina
2 National Scientific and Technical Research Council (CONICET), Av. Rivadavia 1917, C1033AAJ, Buenos Aires, Argentina
3 División de Neurociencia, Centro de Investigación en Complejidad Social (CICS), Facultad de Gobierno, Universidad del Desarrollo, Santiago, Chile
4 Instituto de Ingeniería Biomédica, Facultad de Ingeniería, Universidad de Buenos Aires, Argentina
5 Geroscience Center for Brain Health and Metabolism, Santiago, Chile
6 Memory and Balance Clinic, Buenos Aires, Argentina

Received April 25, 2016. Revised July 4, 2016. Accepted July 19, 2016.

7 National University of La Plata, Physics Institute, (IFLP-CCT-CONICET) La Plata, 1900, Argentina
8 Physics Department, Universitat de les Illes Balears, Palma de Mallorca, Spain
9 Physiopathology Department, ICBM y East Neuroscience Department, Faculty of Medicine, University of Chile, Santiago, Chile
10 Cognitive Neurology and Dementia, Neurology Department, Hospital del Salvador, Santiago, Chile
11 Centre for Advanced Research in Education, Santiago, Chile
12 Neurology Department, Clínica Alemana, Santiago, Chile
13 Center for Social and Cognitive Neuroscience (CSCN), School of Psychology, Universidad Adolfo Ibañez, Diagonal Las Torres 2640, Santiago, Chile
14 Integrative Neuroscience Laboratory, IFIBA, CONICET and Physics Department, FCEyN, UBA, Buenos Aires, Argentina
15 Universidad Torcuato di Tella, Buenos Aires, Argentina
16 Faculty of Elementary and Special Education (FEEyE), National University of Cuyo (UNCuyo), Mendoza, Argentina
17 Universidad Autónoma del Caribe, Barranquilla, Colombia
18 Centre of Excellence in Cognition and its Disorders, Australian Research Council (ACR), Sydney, Australia

Correspondence to: Agustín Ibáñez,
Laboratory of Experimental Psychology and Neuroscience (LPEN),
Institute of Cognitive and Translational Neuroscience (INCyT),
INECO Foundation, Favaloro University, Buenos Aires,
Argentina
E-mail: aibanez@ineco.org.ar

Keywords: social bargaining; social decision-making; self-other strategy; lesion model; neurodegeneration

Abbreviations: AOP = adaptation to other's perspective; ASP = adaptation to self-perspective; bvFTD = behavioural variant frontotemporal dementia; SOIS = self-other integration strategy; VLSM = voxel-based lesion-symptom mapping

Introduction

Social bargaining, as other forms of recursive social decision-making, requires repetitive and flexible long-term strategies for negotiation (Ruff and Fehr, 2014; Lee and Seo, 2016). Involved parties must successively learn to anticipate the other's interests and act strategically to satisfy their own benefits. These skills call on three key processes (Behrens *et al.*, 2009; Lee and Seo, 2016) which escape classical decision-making tasks involving risk or ambiguity. First, an interactive tactic must be developed to maximize self-benefits (Ruff and Fehr, 2014) (adaptation to self-perspective, ASP). Second, interactants must also adapt to the other's preferences and benefits (favouring an adaptation to other's perspective, AOP). Third, and more importantly, integrating their own perspectives with those of others is critical to develop a successful long-term self-other integration strategy (SOIS). This dimension may involve integrative decision values and arbitration among recursive self-other perspectives indexed by the medial prefrontal cortex (Kable and Glimcher, 2009; Nicolle *et al.*, 2012; Donoso *et al.*, 2014), alongside other regions implicated in classical decision-making and social cognition (theory of mind, ToM), as well as areas indexing integration process (such as parietal regions) (Ruff and Fehr, 2014; Hesse *et al.*, 2016; Lee and Seo, 2016). Indeed, different frameworks such as recursive social inferences, the cognitive hierarchy model, model-based reinforcement learning, social valuation models, and adaptive coding posit that complex strategic decisions critically engage fronto-temporo-parietal networks (Seo and Lee, 2012; Stallen and Sanfey, 2013; Ruff and Fehr, 2014; Lee and Seo, 2016). However, the neurobiological foundations of this process during social bargaining are not well understood. Neither is there a clear understanding of whether or how social bargaining is disrupted after frontal damage. To address these issues, we examined neural correlates of strategic bargaining during an ultimatum game with three patient samples and healthy controls.

The ultimatum game is one of the most robust social decision-making paradigms in neuropsychiatric research (Kishida *et al.*, 2010; Sharp *et al.*, 2012; Billeke *et al.*, 2015). In the repeated ultimatum game (or reputation game), the proposer makes offers on how to split a sum of money with another player. From the proposer's perspective, self-serving choices are mixed with socially motivated decisions, as participants have to estimate their actions' risks (a self-centred process) while predicting the other player's decisions (an other-centred process). In other words, social strategic behaviours must be planned to make accurate decisions and achieve interactive goals (Billeke *et al.*, 2014*a*).

Previous research on the ultimatum game has prioritized non-repeated versions, which prevents the study of strategies (Billeke *et al.*, 2014*b*). Moreover, emphasis on the role of the respondent (Seo and Lee, 2012; Stallen and Sanfey, 2013) has hindered the study of offering and negotiation. Against this backdrop, recent iterated versions of the game (Billeke *et al.*, 2013, 2014*a*, *b*) can illuminate how bargainers anticipate their opponents' decisions in complex settings requiring a trade-off between gains and losses. Thus, focusing on the proposer's perspective allows studying ongoing social negotiations throughout a stream of complex decisions.

The neural underpinnings of recursive social decision have been mostly explored through correlational studies

(Ruff and Fehr, 2014) in healthy populations (Sharp *et al.*, 2012) or unspecific psychiatric conditions (Kishida *et al.*, 2010; Sharp *et al.*, 2012; Billeke *et al.*, 2015). Key limitations of the ensuing neuroanatomical insights can be overcome through the lesion model approach, which reveals direct links between affected brain regions and behavioural performance (Rorden and Karnath, 2004). The combination of lesion models, such as stroke and early stage neurodegeneration (Lambon Ralph *et al.*, 2010; Baez *et al.*, 2014*a*; Garcia-Cordero *et al.*, 2015, 2016), offers unique opportunities to understand how specific areas contribute to social bargaining processes. Here, we used this approach focusing on two neurodegenerative conditions [behavioural variant frontotemporal dementia (bvFTD)] and early stage Alzheimer's disease and patients with unilateral frontal lesions partially compromising insular and temporal regions. These conditions may offer novel insights into strategic decisions during social bargaining, as they imply damage to different hubs involved in this dynamic process.

BvFTD is an early onset dementia (Ratnavalli *et al.*, 2002) associated with severe changes in personality (Neary *et al.*, 1998; Rascovsky *et al.*, 2007; Piguet *et al.*, 2011) and social cognition impairments (Ibanez and Manes, 2012; Couto *et al.*, 2013; Baez *et al.*, 2014*a*, *b*, 2016*b*, *c*; Ibanez *et al.*, 2014*b*). It involves damage to the orbitofrontal and medial prefrontal cortices, the insula, and the temporal lobe (Rosen *et al.*, 2002; Brand *et al.*, 2006; Seeley *et al.*, 2009; Piguet *et al.*, 2011; Baez *et al.*, 2014*a*), which are implicated in both social (Lee, 2008; Ruff and Fehr, 2014; O'Callaghan *et al.*, 2016) and non-social (Ernst *et al.*, 2002; Kable and Glimcher, 2009; Gleichgerrcht *et al.*, 2010; Kloeters *et al.*, 2013) decision-making. While previous research on bvFTD has mostly targeted the latter domain (Brand *et al.*, 2006; Gleichgerrcht *et al.*, 2010), recent evidence shows that intact fairness-based decision-making in this condition is accompanied by impaired context sensitivity (O'Callaghan *et al.*, 2016).

Patients with Alzheimer's disease exhibit memory and language deficits but relatively spared social cognition, at least in early disease stages (Cummings and Cole, 2002). Atrophy begins in the medial temporal lobe (hippocampus, parahippocampal cortices) and parietal regions bilaterally (Braak and Braak, 1991; Naggara *et al.*, 2006). The poor performance of patients with Alzheimer's disease in classical decision-making tasks has been associated with memory impairments (Gleichgerrcht *et al.*, 2010). However, these findings are mixed and controversial (Torralva *et al.*, 2000; Sinz *et al.*, 2008; Kloeters *et al.*, 2013).

Frontal lesions are associated with everyday decision difficulties (Clark *et al.*, 2003). The study of social decision following medial prefrontal cortex and specially orbitofrontal cortex lesions shows impaired reasoning about social exchanges (Stone *et al.*, 2002), reduced amount of offers and acceptance rates in the ultimatum game (Koenigs and Tranel, 2007; Krajbich *et al.*, 2009), decreased sensitive to inequity, and failures to integrate social and non-social signals into a decision variable (Moretti *et al.*, 2009). However, while patients with extended frontal damage exhibit risk-taking behaviour, patients with unilateral frontal lesions present more variable performance.

Despite their different underlying neuropathology, bvFTD and frontal lesion patients provide a convergent lesion model to assess the critical frontal regions involved in SOIS. Moreover, the combined study of two frontal disorders together with Alzheimer's disease, whose structural degeneration is associated with posterior parietal and temporal regions, gave us the unique opportunity to investigate how different brain areas influence diverse aspects of long-term social negotiation. Indeed, while previous findings have shown that different frontal regions (Bhatt *et al.*, 2010; Lee and Seo, 2016) as well as posterior parietal and temporal structures (Coricelli and Nagel, 2009; Billeke *et al.*, 2013, 2014*b*) play an important role during social bargaining, no studies have investigated strategic negotiation in these patients.

The investigation of real time brain dynamics during social decision-making in stroke and neurodegeneration is very rare. Studies in healthy populations have shown that oscillatory theta/alpha/beta activity at frontal and temporo-posterior regions is associated with control and conflict monitoring in social interactions (Billeke *et al.*, 2013; Cristofori *et al.*, 2013). In the repeated ultimatum game, the power of alpha/beta activity predicts the risk of the proposer's offers and anticipates others' decisions (Billeke *et al.*, 2013). Moreover, alpha/beta activity predicts strategic long-term adaptations in social interactions (Billeke *et al.*, 2014*a*). Thus, anticipatory activation to risk, indexed by alpha/beta oscillations, constitutes a dynamic brain correlate of social bargaining.

Previous imaging reports of social decision-making have shown distributed involvement of frontal, temporal, and parietal regions (Vickery *et al.*, 2011), suggesting that these correlates may depend on inputs from and interaction with distinct brain networks (Seo and Lee, 2012; Ruff and Fehr, 2014). Similarly, connectivity studies have revealed that regions associated with social and non-social decisions within fronto-temporo-parietal networks (Cocchi *et al.*, 2013; Cole *et al.*, 2013; Janowski *et al.*, 2013) are engaged in social choices (Ruff and Fehr, 2014) and prove flexible to task demands (Cole *et al.*, 2013). Complex social interaction strategies depend on switching among self and others' perspectives (Stallen and Sanfey, 2013), which also calls on large-scale brain networks (Cocchi *et al.*, 2013). The circuit underlying prosocial actions may overlap with structures involved in computing subjective value and decision-making (Delgado *et al.*, 2005; Zaki and Mitchell, 2011; Stallen and Sanfey, 2013; Ruff and Fehr, 2014; O'Callaghan *et al.*, 2016). Yet, evidence is scant on how these processes interact in complex and interactive social bargaining.

In this work we adopted a multilevel approach to analyse social bargaining at different spatial and temporal brain scales. Bringing together multidimensional tools is a key

step towards obtaining a larger picture of complex brain properties (Devor *et al.*, 2013). In particular, the use of a task indexed with various brain measures may reveal different spatial and temporal mechanisms involved in the same process (Garcia-Cordero *et al.*, 2015, 2016; Melloni *et al.*, 2015). Here, using three different lesion models and combining structural and functional imaging as well as ongoing brain temporal dynamics, we tested the crucial role of frontal hubs and related networks during recursive social interactions. As stated above, recent research assessing social decision-making in bvFTD has shown preserved performance in basic normative behaviour but altered integration of more complex social contextual information associated with reduced grey matter volume in several prefrontal structures (O'Callaghan *et al.*, 2016). In the same vein, evidence from patients with ventromedial prefrontal lesions has revealed intact self-interest and fairness-based decisions alongside impairments in adaptation to long-term consequences (Moretti *et al.*, 2009). Consequently, at behavioural level, we anticipated a relative preservation of basic processes (ASP, AOP) in all groups, but an impaired bargaining strategy (SOIS) in frontal disorders (bvFTD and frontal lesions). At a structural level [voxel-based morphometry, and voxel-based lesion-symptom mapping (VLSM)], we predicted associations between prefrontal regions engaged in strategic decisions (e.g. orbitofrontal cortex and, more broadly, medial prefrontal cortex) for SOIS. Moreover, given that alpha/beta activity predicts strategic long-term adaptations in social interactions, we hypothesized that our control group would corroborate this finding. More particularly, since large-scale brain networks have been associated with the ability to integrate both self-related and vicarious choices during social interaction (Decety *et al.*, 2004; Hampton *et al.*, 2008; Hare *et al.*, 2010; Janowski *et al.*, 2013; Smith *et al.*, 2014), we expected functional connectivity analyses to reveal a large-scale network indexing SOIS. This network, cutting across fronto-temporo-parietal regions involved in social cognition, decision-making, and integration processes, should also be distinctively compromised in frontal disorders (bvFTD and frontal lesions).

In sum, social bargaining has been hitherto studied piecewise and in correlational studies. This is the first study simultaneously measuring all potential signatures (behavioural variance, brain integrity, oscillations, brain networks) of social negotiation in contrastive lesion models. Joint consideration of these markers offers an unprecedented window into the multidimensional underpinnings of social bargaining, regions from the contribution of single regions to global network interactions.

Materials and methods

Participants

We recruited three patient samples totalling 85 participants.

Patients with bvFTD ($n = 26$) were diagnosed following current revised criteria (Rascovsky *et al.*, 2011). BvFTD is an early onset dementia (Ratnavalli *et al.*, 2002) associated with fronto-temporo-insular atrophy on MRI (or frontal hypoperfusion in PET recordings). BvFTD patients presented with functional impairment and prominent changes in personality and social behaviour as verified by a caregiver during initial assessment. We excluded all patients who gave signs of other forms of dementia (e.g. primary progressive aphasia and amyotrophic lateral sclerosis). The resulting sample offers a unique model of fronto-insular compromise, which includes critical areas for social decision-making.

Patients with Alzheimer's disease ($n = 21$) were diagnosed following NINCDS-ADRDA criteria (McKhann *et al.*, 1984, 2011). These patients present with memory deficits and earlier atrophy in the temporal lobes, parietal regions (Braak and Braak, 1991; Naggara *et al.*, 2006), and, in some cases in the insula cortex (Bonthius *et al.*, 2005). Patients with logopenic progressive aphasia and atypical forms of Alzheimer's disease (e.g. posterior cortical atrophy), were not included. The posterior atrophy characteristic of Alzheimer's disease provides an alternative model relative to frontal neurodegeneration in bvFTD. This model thus allowed us to explore other areas (e.g. hippocampus, temporal pole, parietal regions) likely to be implicated in specific decision-making dimensions.

Patients with frontal lesions presented with non-haemorrhagic, fronto-insular lesions provoked by stroke. They were evaluated at least 6 months post-stroke (the time needed for stability of the lesion and presentation of clinical symptoms). A direct comparison of these patients with bvFTD patients (Baez *et al.*, 2014*a*; Garcia-Cordero *et al.*, 2015, 2016) may reveal convergent areas that contribute to decision-making dimensions (which may or not be differentially compromised by the distinctive aetiology of each condition).

We also assessed 22 healthy control subjects matched for age, gender, handedness, and education (Supplementary material). All patients underwent a standard examination including neurological, neuropsychiatric, and neuropsychological measures and a clinical MRI scan. Additional evaluations ruled out specific psychiatric disorders in all patients. For further details about diagnosis and assessment, see Supplementary material.

Before the study, all participants read and signed an informed consent form in accordance with the Declaration of Helsinki. The study's protocol was approved by the institutional Ethics Committee of all involved centres.

Neuropsychological assessment

The patients' cognitive state was assessed through the Addenbrooke's Cognitive Examination (ACE-III) (Mioshi *et al.*, 2006), which includes the Mini-Mental State Examination (MMSE) (Folstein *et al.*, 1983). Executive functions were assessed with the INECO Frontal Screening (IFS) battery, which taps eight relevant domains (Torralva *et al.*, 2009). The Hayling test was used to measure inhibitory control (Burgess and Shallice, 1996).

Social bargaining: behavioural task

Participants played as 'proposers' in a previously tested repeated version of the ultimatum game (Billeke *et al.*, 2013, 2014*a*, *b*, 2015) (Fig. 1A). Participants were told they would

play with a human partner, but they actually faced a simulated partner (detailed below). Task instructions emphasized that the participant's partners would play independently of each other, with no collusion. All participants played a probe game with the experimenter to become familiar with the setting. At the beginning of each game, participants watched a fixation cross (10 s, fixation phase) and then a video of their partner. All videos showed full, coloured faces of participants on a black background. Participants played eight 20-round games, each against a different responder. Each trial had three phases: (i) an offer phase of variable duration, in which the proposer had to make the offer; (ii) an anticipation phase (1.5–4 s), in which the proposer waited for the partner's response; and (iii) a feedback phase (1 s), in which the response was revealed. At the end of each game, the players' scores were revealed. The amount of money each participant received depended on his/her performance in a randomly chosen round.

The simulation's probability to accept or reject the offer was obtained from a mixed logistic model of people playing as receptors with other people (for details see Billeke *et al.*, 2013). This model allowed creating different virtual players. Specifically, the simulation assigns a probability to reject or accept the offer given the following two equations:for round (x) = 1

$$logit(R_x) = (b_0 + r_0{}^i) + (b_1 + r_1{}^i)O_x \quad (1)$$

and for round $(x) > 1$

$$logit(R_x) = (b_0 + r_0{}^i) + (b_1 + r_1{}^i)O_x + (b_2 + r_2{}^i) \quad (2)$$

where *logit* (R_x) is the logit transform of the probability of rejection for the round x, O_x the offer, ΔO_x the change of offer in relation to the preceding offer, and Pr_x the preceding response. The coefficients estimated for each regressor were composed by a population parameter (b_y) and a random effect for each simulated responder (r_{yi}, y = regressor, and i = simulated partner). The *logit* (R_x) was used to quantify the risk per each offer made. For further details, see Supplementary material.

Dynamical changes and long-term strategies favouring the player or the partner were indexed by three scores (Fig. 1B–D).

Adaptation to self-preferences

This measure focuses on the tendency to decrease the offer when an acceptance occurs, reflecting a basic strategy that benefits one's own perspective. It is computed as the mean of the delta between the previous accepted offer and the following one. Negative values are expected for good players.

For $Response_{r-1}$ = Acceptances

$$ASP = \frac{1}{n}\sum_{n}^{r=2} O_r - O_{r-1} \quad (3)$$

Where O_r is the offer made in round r, and O_{r-1} is the offer made in round r–1. For this calculation we considered only the offer change $(O_r - O_{r-1})$ when an acceptance occurred in O_{r-1}. The rounds range between 2 to 20, for the each of the eight games.

Adaptation to others' preferences

This measure focuses on how participants change their offer after a rejection, reflecting the adaptation to others' preferences as evidenced in one's own decisions. It is computed as the mean of the delta between the previous rejected offer and the following one. Positive values are expected for good players.

For $Response_{r-1}$ = Rejection

$$AOP = \frac{1}{n}\sum_{n}^{r=2} O_r - O_{r-1} \quad (4)$$

Where O_r is the offer made in round r, and O_{r-1} is the offer made in round r-1. For this calculation we considered only the offer change $(O_r - O_{r-1})$ when a rejection occurred in O_{r-1}. The rounds range between 2 to 20, for the each of the eight games.

Self-other integration strategy

This measure captures the evolution of players' long-term strategies considering the offers and the integration of AOP and ASP. It is computed as the individual correlation between the round number and the logit transform of the simulation's probability to accept the offer. This index represents the integration of both self-preference and other-preference processes in long-term strategic behaviour throughout the games (Billeke *et al.*, 2013). Thus, it captures a global tendency in each subject's evolving strategy during negotiation, beyond local reactivity to a rejection or an acceptance (which represents the short-term variations inherent to the bargaining). In other words, SOIS represents the way in which subjects reach agreement with their partners during each game. Thus, greater SOIS values indicate that subjects integrate the other preferences to obtain more acceptances, while smaller SOIS values indicate that the proposer maintains a fixed strategy independently of the other's preferences. This measure was obtained by averaging the logit of the first offer of all games, then that of the second offer of all games, and so on, per each subject, and then calculating the Spearman's correlation between this mean logit offer and the corresponding round number. Then, the rho value (SOIS) was obtained as follow:

$$rho = corr\left(Logit_{g=meanr=[2,20]}, Roundnumber_{[2,20]}\right) \quad (5)$$

The first offer was not used, as the algorithm that the simulation uses to calculate the logit lacks a parameter relate to the preceding round. We assessed the Spearman's correlation since prior work evidenced an inconclusive linear relationship between these parameters (see below), showing a tendency towards stability of the offer risk during the last offers of each game (Billeke *et al.*, 2014*b*). Note that here we used 20-round games to maximize data from the part of the game with greater slope. Prior work has shown that this index can distinguish between clinical and healthy samples (Billeke *et al.*, 2015).

Thus, both AOP and ASP represent local adaptation in short-term bargaining interaction, whereas SOIS represents the long-term flexibility (or absence thereof) needed to reach an agreement (or not) during a recursive social interaction. For details, see online Supplementary material.

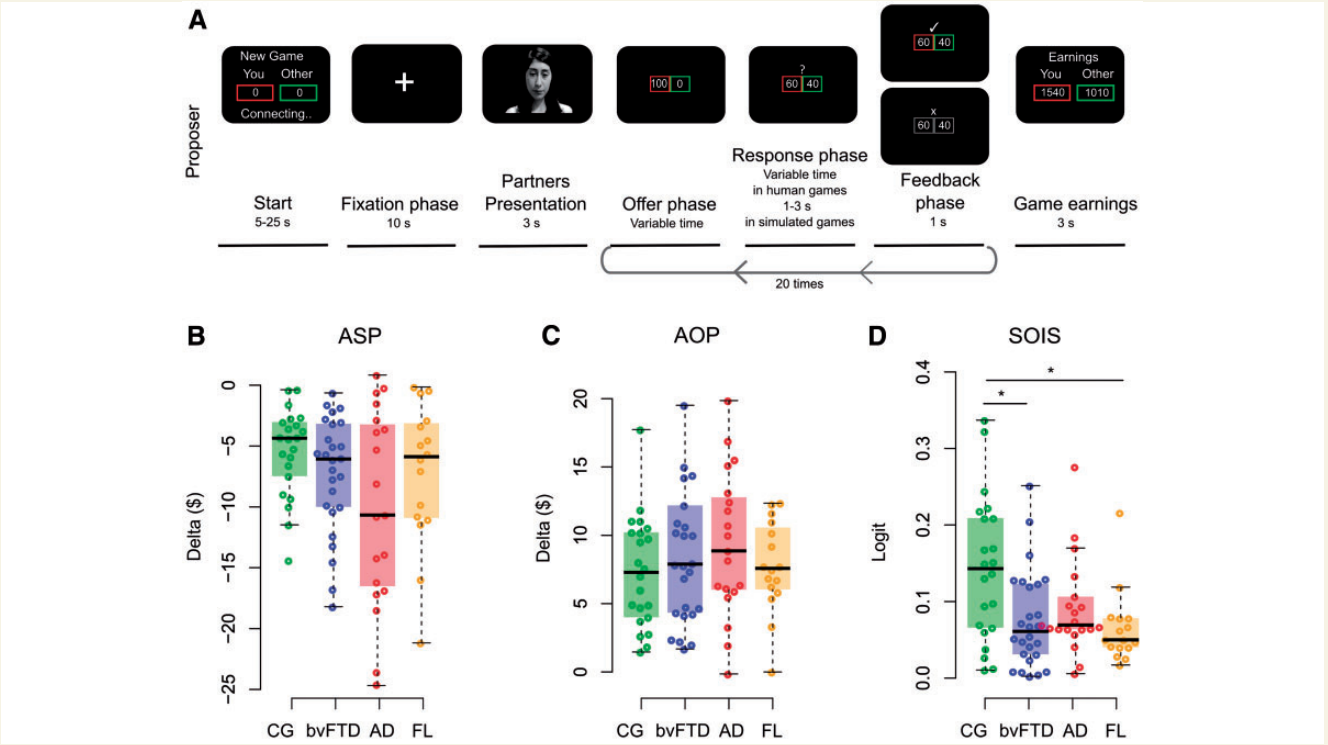

Figure 1 Behavioural indexes. (**A**) Timeline for a game. Proposers (red box) and responders (green box) played an iterated ultimatum game in different rooms. At the beginning of each game, participants watched a fixation cross (10 s, fixation phase) and then a video of their partner. The proposer made an offer on how to split 100 points between the responder and himself (offer phase). The responder saw the offer and accepted or rejected it (response phase). If the responder accepted the offer, the money was split as proposed; if he/she rejected it, the money was lost. The response was shown on the screen for 1 s (feedback phase). Each game consisted of 20 iterated offers. In the EEG study, proposers believed that they were playing with a human partner, but they were actually playing with a simulation based on the behavioural study. The original screens were in Spanish. (**B**) Adaptation to self-preference (ASP). Offering behaviour related to an acceptance separated by group. No significant differences between groups were found in these indexes. (**C**) Adaptation to other's preference (AOP). Offering behaviour related to rejection separated by group. No significant differences between groups were observed in these indexes. (**D**) Self-other integration strategy (SOIS). Individual correlation between the round number and the logit transform of the probability that the simulation will accept the offer. Significant difference between controls and bvFTD and between controls and frontal lesions patients. (**B–D**) Circles represent subjects, broken lines represent the medians, and rectangles represent the interquartile segment. Green represents the healthy controls, blue represents patients with bvFTD, red represents patients with Alzheimer's disease, and orange represents patients with frontal lesions. $^{*}P < 0.05$. Intra-group analyses were performed with Wilcoxon's signed rank test; comparisons among groups were calculated with Kruskal-Wallis test, *post hoc* analysis were conducted with Dunn's test. CG = control group; AD = Alzheimer's disease; FL = frontal lesion.

Additional measures

Finally, we used two basic control measures, indexing basic normative risk adjustment (first offer) and consistency of the offers (the standard deviation of the offer through the rounds of each game). For further details, see Supplementary material.

MRI recordings

MRI recordings were obtained with a 1.5 T Phillips Intera scanner equipped with a standard head coil. A T_1-weighted spin echo sequence acquired parallel to the plane connecting the anterior and posterior commissures and covering the whole brain was used to generate 120 contiguous axial slices (repetition time = 2300 ms; echo time = 13 ms; flip angle = 68°; field of view = rectangular 256 mm; matrix size = 256 × 240; slice thickness = 1 mm). Additional images were obtained during a 10-min functional MRI resting protocol, where participants were asked not to think about anything in particular, to keep eyes closed, and to avoid moving or falling sleep. Functional images were acquired on a 1.5 T scanner with an eight-channel skull coil. Thirty-three (5-mm thick) axial slices were parallel to the plane of conjunction of the anterior and posterior commissures, covering the entire brain (repetition time = 2777 ms; echo time = 35 ms; angle = 90; volumes = 209 units).

EEG recordings

EEG signals were recorded online while participants performed the ultimatum game with a 129-channel Biosemi system at 1024 Hz. We followed the same preprocessing procedures as reported in previous works of our group (Billeke *et al.*, 2013, 2014*a*, *b*, 2015). For preprocessing details, see Supplementary material.

Data analysis

Demographic and neuropsychological data were compared through one-way ANOVAs, while categorical variables (e.g. gender) were analysed using chi-square tests.

Behavioural measures

All behavioural statistical analyses were performed in R. As most game variables did not meet the normality assumption (Billeke *et al.*, 2013, 2014*a*, *b*, 2015), we used non-parametric tests. Intra-group analyses were performed with Wilcoxon's signed rank test. Comparisons among groups were calculated with the Kruskal Wallis test, and *post hoc* analyses were conducted with Dunn's test.

Voxel-based morphometry analysis

Images were preprocessed using the DARTEL Toolbox, following previously described procedures (Ashburner and Friston, 2000). Then, modulated 12-mm full-width at half-maximum kernel-smoothed images (Good *et al.*, 2001) were normalized to the MNI space and analysed using general linear models for second-level analyses using SPM-12 software. To identify the areas of grey matter atrophy in bvFTD and patients with Alzheimer's disease [(Couto *et al.*, 2013), Figs. 2A and 2B, respectively], two-sample comparisons between each group of patients and controls were performed, including the total intracranial volume as a confounding covariate [whole brain analysis, $P < 0.001$, uncorrected, extent threshold = 100 voxels (Irish *et al.*, 2014*b*)]. We used the SPM multiple regression module to determine brain regions in which grey matter volume was associated with SOIS (Fig. 3A–F). Correlations between SOIS index and regions of grey matter volume were investigated in bvFTD and patients with Alzheimer's disease independently. Both patients and controls were included in each analysis (bvFTD and Alzheimer's disease), to increase behavioural variance and statistical power (Sollberger *et al.*, 2009; Irish *et al.*, 2014*a*; O'Callaghan *et al.*, 2016). For all regression analyses, we considered total intracranial volume and ACE-III total scores as covariates of no interest. The statistical threshold was defined as $P < 0.001$ (extent threshold = 50 voxels). In addition, to investigate potential convergences among the three groups within the affected regions, we performed a more restrictive analysis. We derived a mask from previous results including the regions with significant association between SOIS scores and grey matter volume (in bvFTD and Alzheimer's disease) as well as between SOIS scores and damaged voxels (in frontal lesions). Then, using this mask, we performed multiple regression analyses for each group [$P < 0.05$, false discovery rate (FDR) corrected, see Supplementary Fig. 3].

Lesion mapping

Lesions were first manually mapped by two trained investigators in MRIcron software. These maps were normalized to a standard template using the statistical parametric mapping-12 software with cost-function masking. The lesions were further analysed in terms of lesion overlaps with MRIcron. Lesion overlap across patients was mapped on a standard brain (Fig. 2C).

We applied VLSM to test for lesion–behaviour associations (Bates *et al.*, 2003) (Fig. 3G and H). Performance on the ACE-III was regressed out as in previous studies using VLSM (Han *et al.*, 2013; Henseler *et al.*, 2014; Almairac *et al.*, 2015). The statistical threshold was defined as $P < 0.001$ (extent threshold = 50 voxels). In VLSM, the performance measure of interest is entered as a continuous measure, and statistical comparisons are made for each eligible voxel, comparing the performance of subjects with damage affecting a given voxel with that of subjects with damage outside that voxel. To avoid the multiple comparison problem, a non-parametric mapping was conducted using the Brunner and Munzel permutation test (Brunner and Munzel, 2000) with 5000 permutations ($P < 0.05$). Following previous reports (Falquez *et al.*, 2014), we used the NPM module of MRIcron (Rorden *et al.*, 2007) to generate non-parametric tests.

EEG analysis

During assessment we inadvertently lost one-third of the recordings, due to damage in a cable transmitting the TTL (transistor–transistor logic) pulses. Of the remaining subjects, only 40 complied with our analysis requirements: strong signal-to-noise ratio and $<30\%$ of rejected trials [13 controls, 13 bvFTD, seven Alzheimer's disease, and seven frontal lesions; see Ibanez *et al.* (2012, 2014*a*) and Supplementary material for further details]. We focused on oscillatory activity of the anticipation phase (when subjects anticipate the other player's decision), as such a property reveals power modulations in the alpha/beta band during human games (Billeke *et al.*, 2014*a*) and differentiates psychiatric patients with social cognition impairments (Billeke *et al.*, 2015). Given that oscillation analysis provides an ongoing, dynamic brain measure, while SOIS reflects a long-term strategy measure, we used the risk variable which has already been demonstrated to modulate the trial-by-trial strategic behaviour (Supplementary material). For each subject, we first fitted a generalized linear model (GLM) of the power of the oscillatory activity per trial (first-level analysis) using as regressor the logit of the probability to acceptances. We obtained a 3D matrix of *t*-values (sensor, time, frequency) for each regressor and subject. We then explored differences within and between groups using the Wilcoxon test (second-level analysis). To correct for multiple comparisons in time-frequency charts, we used a cluster-based permutation test (Maris and Oostenveld, 2007).

Source estimation

By applying a weighted minimum norm estimate inverse solution (Baillet *et al.*, 2001) with unconstrained dipole orientations in single-trials (Gonzalez-Gadea *et al.*, 2015) we estimated the neural current density time series at each elementary brain location. We used individual head models based on individual surfaces (pial, inner skull, and scalp) to calculate the current source distribution. Then, the result of each cortical surface was normalized to a standard default anatomy surface (Colin 27 from McConnell Brain Imaging Centre, Montreal Neurological Institute, McGill University, Montreal, Quebec). See Supplementary material for further details.

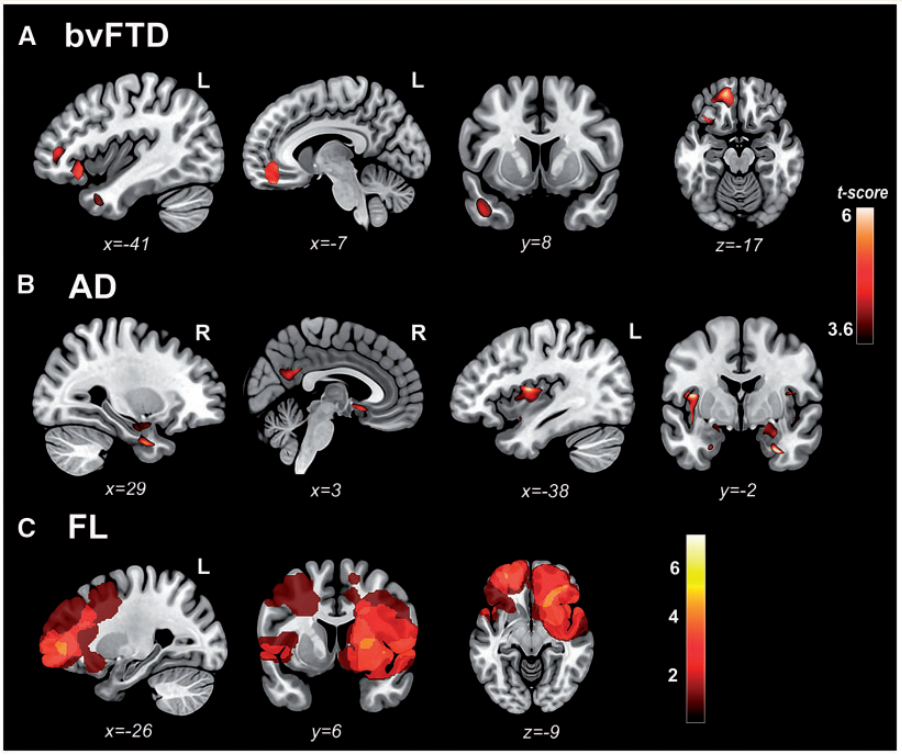

Figure 2 Voxel-based morphometry results. (**A**) Cluster of significant grey matter volume atrophy of the superior orbitofrontal cortex, the middle superior frontal gyrus, the inferior orbitofrontal cortex, the inferior frontal gyrus, and the middle temporal gyrus of bvFTD patients compared to controls. (**B**) Cluster of significant grey matter volume atrophy of the hippocampus and parahippocampus, the precuneus, the posterior cingulate cortex, the insula, and the posterior temporal regions (see also Supplementary Table 2) of patients with Alzheimer's disease compared to controls. (**C**) Lesion overlap across frontal lesions patients (frontal and insular structures). Main overlap is in prefrontal cortex, with secondary damage in the putamen, insula, the temporal poles, and other frontal regions. R = right; L = left. AD = Alzheimer's disease; FL = frontal lesion.

Functional imaging and brain connectivity analyses

First, functional images were tested on the Artifact Repair toolbox for SPM8 to improve analysis of high-motion subjects (Mazaika *et al.*, 2009, Garcia-Cordero *et al.*, 2015). This toolbox automatically detected noise in the raw data. Images showing >0.5 mm/repetition time were interpolated to avoid large outliers from propagating to valid data (Bruno *et al.*, 2014). In no subject did $>20\%$ of functional MRI series volume require repair. We excluded participants showing head movements >3 mm and/or rotation movements higher than 3° (Supekar *et al.*, 2008), namely: three controls, six bvFTD patients, three patients with Alzheimer's disease, and one patient with frontal lesions. Then, we compared the mean translational and mean rotational parameters among groups using an ANOVA test. No differences were found among groups (Supplementary Table 4).

Following previously reported procedures in stroke and neurodegeneration (Garcia-Cordero *et al.*, 2015, 2016; Sedeño *et al.*, 2015), images were preprocessed using the Data Processing Assistant for Resting-State functional MRI (DPARSF) (for further details see Supplementary material).

Regarding matrix construction, based on the Automated Anatomical Labeling (AAL) atlas (Tzourio-Mazoyer *et al.*, 2002), mean time courses were extracted by averaging the blood oxygenation level-dependent signal of all voxels contained in each of the 90 regions of interest. Pearson's correlation coefficient was used to construct a 90-node functional connectivity network for each subject from these time series. Given that negative correlations in resting functional MRI are still a controversial issue and considered less systematic (Rubinov and Sporns, 2010; Sporns, 2013), we discarded anti-correlations for subsequent analysis that are based on these connectivity matrices.

The connectivity analysis was implemented to study the information broadcasting between different regions and their association with SOIS scores in all groups. Whole-brain Spearman correlation analysis (Garcia-Cordero *et al.*, 2015; Sedeño *et al.*, 2015) was used to determine the functional network associated with SOIS across groups. We applied two strategies to control the multiple comparisons that arise in associating multiple connections and SOIS: first, we implemented a false discovery rate correction (FDR, $P < 0.05$) (Benjamini and Hochberg, 1995); then, using the connections that survived this correction, we selected only strong correlation values (e.g. rho > 0.35; Fig. 5A). This ensured that the resulting network was comprised of the most significant and important connections.

The brain network associated with SOIS (network estimated from all subjects) was expected to involve large-distance network integration (e.g. frontal, temporal, parietal) of different

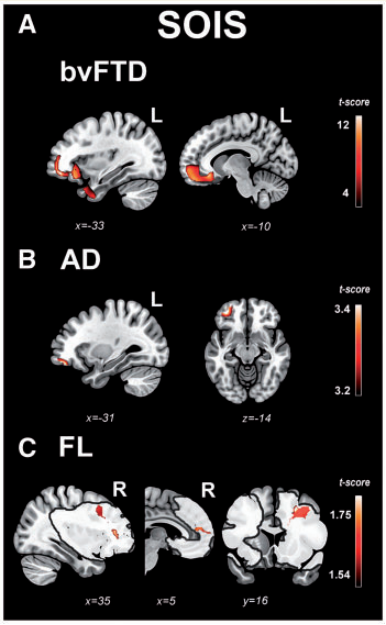

Figure 3 Structural brain correlates of social bargaining including ACE-III and total intracranial volume as covariates. (**A**) Structural correlation between grey matter volume in the left middle and inferior orbitofrontal gyri, the left rectal gyrus, the left temporal pole, and the left fusiform gyrus, and SOIS scores in bvFTD. (**B**) Structural correlation between grey matter volume in the left middle orbitofrontal gyrus and SOIS scores in Alzheimer's disease. (**C**) Structural correlation between the damaged voxels in the right superior and right middle frontal gyri, the right portions of the pars opercularis and pars triangularis of the inferior frontal gyrus, the right part of the superior medial frontal gyrus and SOIS scores in frontal lesions. The regions identified with a lighter mask correspond to damaged areas. AD = Alzheimer's disease; FL = frontal lesion.

social and non-social decision-making processes (Decety *et al.*, 2004; Hampton *et al.*, 2008; Hare *et al.*, 2010; Janowski *et al.*, 2013). To evaluate how connectivity decays with distance (Garcia-Cordero *et al.*, 2015), we used an interregional distance analysis within the network estimated from all subjects. By considering short, middle, and long spatial ranges in connectivity, we aimed to reveal aetiology-specific patterns of regional functional connectivity at small, medium, and large levels. First, we classified the connections as long (two-thirds or more than maximal distance value), medium (between one- and two-thirds of maximum value), and local (shorter than one-third of maximal distance among groups) range. See Supplementary Table 5 for details about range distances and the number of links included into each range, by groups.

Then, we considered the strongest connections within the network estimated from all subjects for each group (those with a correlation value >0.35 relative to the each group's mean network). For each group these connections were identified as short, middle, and long (distanced connections). Finally, for each subject within the specific group, we derived an index from the number of these distanced connections weighted based on their connectivity strength within the network estimated from all subjects. Using a Monte Carlo permutation test (10 000 permutations) combined with bootstrapping (Nichols and Holmes, 2002), we compared this index of each distanced connection between groups (Fig. 5B).

We also generated a SOIS network estimated from the controls' values (network estimated from control subjects), using the same procedure used to estimate the SOIS from all subjects. This analysis was centred in fronto-temporo-parietal regions. Moreover, we distinguished among long, medium, and local-range connections using a Monte Carlo permutation test combined with bootstrapping (same procedure used in the network estimated from all subjects). Also, to characterize the network pattern associated with adequate SOIS performance, we compared the spatial range of connections between groups exhibiting good (controls, Alzheimer's disease) and bad (bvFTD, frontal lesions) performance for both networks (network estimated from all subjects and network estimated from controls subjects).

Results

Demographic and neuropsychological data

No significant differences in age, gender, or education were observed among controls and each group. As expected, all patient groups presented lower levels of executive functions. For statistical details about demographic and neuropsychological variables for bvFTD, Alzheimer's disease, frontal lesion patients, and controls see Supplementary material.

Behavioural results

Offering behaviour related to rejections and acceptances was evaluated in all groups. We separately considered basic measures (ASP and AOP) and long-term strategies (SOIS).

Adaptation to self-perspective

All participants tended to decrease their offer when an acceptance occurred (Wilcoxon, $P < 0.001$, for all groups; controls: $V = 0$, $P = 4.768 \times 10^{-7}$; bvFTD: $V = 0$, $P = 2.98 \times 10^{-8}$; Alzheimer's disease: $V = 3$, $P = 1.907 \times 10^{-5}$; frontal lesions: $V = 0$, $P = 3.052 \times 10^{-5}$; Fig. 1B), reflecting preserved self-oriented adaptation. We did not find differences between groups (Fig. 1B) in these indexes (Kruskal-Wallis chi-squared = 0.786, df = 3, $P = 0.78$).

Adaptation to other's perspective

Figure 1C shows that both control and clinical groups increased their offer when a rejection occurred, reflecting preserved adaptation to the other's perspective (Wilcoxon, $V > 120$, $P < 0.001$ for all groups; controls: $V = 253$, $P = 4.768 \times 10^{-7}$; bvFTD: $V = 351$, $P = 8.796 \times 10^{-6}$; Alzheimer's disease: $V = 231$, $P = 7.629 \times 10^{-6}$; frontal lesions: $V = 120$, $P = 0.0007$). No differences between groups

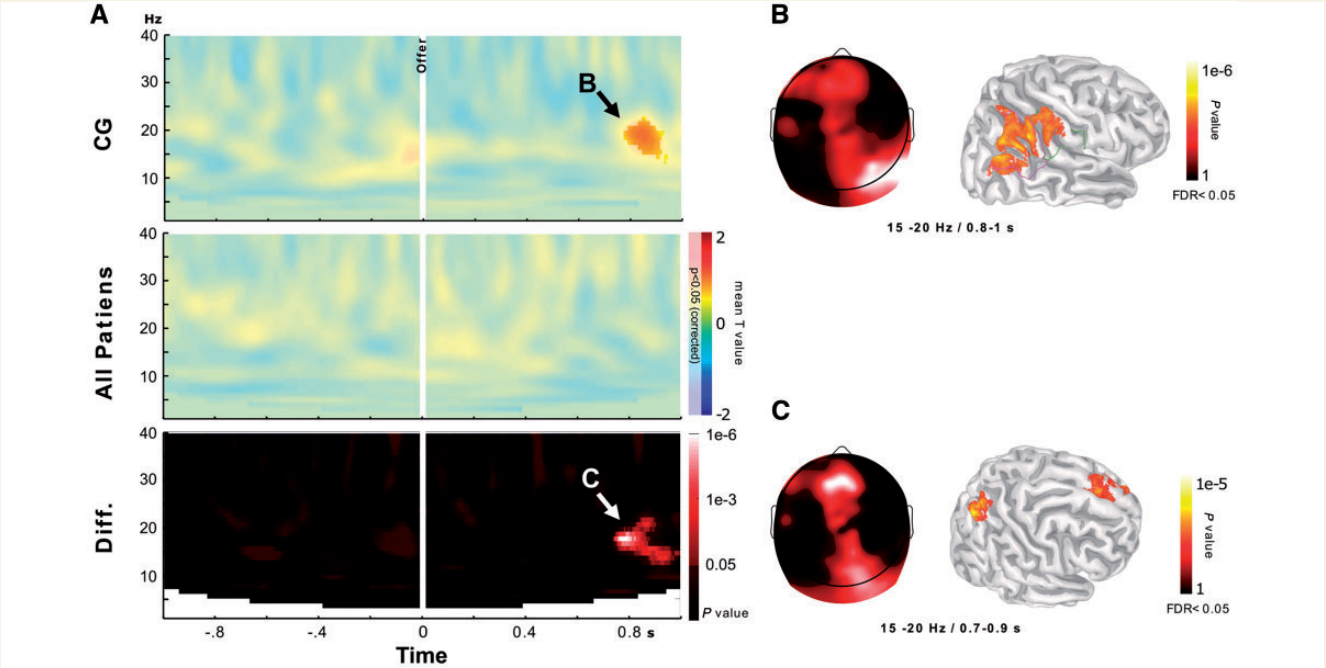

Figure 4 Oscillatory correlates of social bargaining. (**A**) Time-frequency chart of controls, all patients, and the difference between controls and all patients during the ultimatum game. Colours represent the mean across subjects of the *t* value of the individual correlation between the power of the oscillatory brain activity and the risk of the offer made. The clusters of significant effects are highlighted ($P < 0.001$ cluster-corrected). (**B**) Topographic distribution and source estimation of significant cluster of alpha/beta activity after the offer (15–20 Hz, 0.8–1 s) in controls. (**C**) Topographic distribution and source estimation of significant cluster of alpha/beta activity after the offer (15–20 Hz, 0.7–0.9 s) in the contrast between controls and all patients. For each group comparison, see Supplementary Fig. 2. CG = controls.

were observed (Kruskal-Wallis chi-squared = 0.186, df = 3, $P = 0.98$).

Self-other integration strategy

We evaluated the evolution of long-term offer strategies computing the individual correlation between the probability to acceptances and the round number (Fig. 1C). We found significant differences among groups (Kruskal-Wallis chi-squared = 10.3, $df = 3$, $P = 0.015$). Dunn's test *post hoc* analysis revealed that, compared to controls, both bvFTD ($P = 0.047$) and frontal lesions ($P = 0.045$) presented lower SOIS indexes. No difference was found between Alzheimer's disease and controls.

Finally, regarding non-specific measures of social bargaining, we found that Alzheimer's disease presented reduced normative risk adjustment (significantly lower first offer) than controls. In addition, the consistency of the offer was reduced in both Alzheimer's disease and bvFTD (greater variation of the offer throughout rounds) when compared with controls (Supplementary Fig. 1 and Supplementary material).

Considering that: (i) ASP and AOP performance was preserved in all clinical groups; (ii) SOIS was the most relevant index of social bargaining as it allowed evaluation of the deployment of dynamically evolving strategies in their offers across rounds; and (iii) SOIS was the only measure impaired in bvFTD and frontal lesions, we focused on the neural correlates of the strategic decision index.

Voxel-based morphometry

Supplementary Tables 1 and 2 provide the coordinates of peak voxels in clusters showing significant grey matter reduction in patients with bvFTD and Alzheimer's disease.

Behavioural variant frontotemporal dementia brain atrophy

Compared to controls, bvFTD patients showed frontotemporal atrophy (one cluster in the frontal lobes included the superior orbitofrontal cortex and the middle superior frontal gyrus). Atrophy was also observed in the inferior orbitofrontal cortex, the inferior frontal gyrus, and the middle temporal gyrus (Fig. 2A and Supplementary Table 1). This atrophy pattern is consistent with that reported in previous studies (Rosen *et al.*, 2002; Kipps *et al.*, 2009; Seeley *et al.*, 2009; Whitwell *et al.*, 2009).

Alzheimer's disease brain atrophy

In the voxel-based morphometry analysis, patients with Alzheimer's disease showed an expected volume loss mainly comprising hippocampus and parahippocampus, precuneus, posterior cingulate cortex, the insula, and posterior temporal regions, among others (Fig. 2B and

Supplementary Table 2). These atrophy patterns replicate previous results (Lerch *et al.*, 2005; Du *et al.*, 2007; Ferreira *et al.*, 2011).

Brain structural correlates of social bargaining

Supplementary Table 3 summarizes the coordinates of peak voxels in significant clusters associating SOIS behavioural scores to grey matter volumes of bvFTD and Alzheimer's disease. In bvFTD, the SOIS correlated with grey matter volume in the left orbitofrontal gyri, the left rectal gyrus, and the left temporal pole (Fig. 3A). In Alzheimer's disease, this score was associated with grey matter volume in the left middle orbitofrontal gyrus (Fig. 3B). In frontal lesions, this score was associated with damaged voxels in the right superior and right middle frontal gyri, the right portions inferior frontal gyrus and the ventromedial prefrontal cortex (Fig. 3C). Moreover, masking analysis results replicated those obtained in whole-brain analysis for all groups, additionally revealing an overlap within the ventromedial prefrontal cortex in both bvFTD and frontal lesions (Supplementary Fig. 3).

Oscillatory correlates of social bargaining

We analysed oscillatory brain activity while subjects participated in the ultimatum game. We focused on the anticipation phase, when subjects have to anticipate the others' player to estimate how risky the proposal they had just made was (Billeke *et al.*, 2013). As expected, risky offers in controls modulated alpha/beta activity 800–1000 ms after the offer (Fig. 4B, cluster-based permutation test, $P < 0.001$). This modulation was observed mainly in a right temporo-parietal region, and in fronto-central scalp. Source estimation revealed that this activity came mainly from right temporo-parietal junction (including both the inferior parietal lobe and the supramarginal gyrus, Wilcoxon-test and FDR $q < 0.05$). Interestingly, comparing with the clinical group, we found significant differences in this time-frequency window. When compared with a single collapsed clinical group, differences to control subjects were found mainly in right posterior and fronto-central regions, although single patients group comparison revealed differences with bvFTD and frontal lesions only (the source space included the superior parietal lobe and the superior frontal gyrus, Wilcoxon-test and FDR $P < 0.05$, Fig. 4C). Analyses for each group are presented in the Supplementary material and Supplementary Fig. 2.

Moreover, the alpha/beta band in temporo-parietal scalp predicted SOIS of each subject in the control group (rho = 0.6154, $P = 0.02$). As previously shown in other neuropsychiatric populations (Billeke *et al.*, 2015), this association was not significant in the clinical groups (rho = −0.23, $P = 0.27$, difference between correlations: $Z = 2.53$, $P = 0.01$). As ventromedial prefrontal cortex volume correlated with SOIS, we assessed the ratio between these three variables using partial correlation. We found that alpha/beta independently correlated with both volume of ventromedial prefrontal cortex (Spearman's partial correlation rho = 0.6041, $P = 0.038$) and SOIS (rho = 0.7393, $P = 0.006$).

Functional connectivity

The analysis of the association between functional connectivity and the SOIS index across groups revealed a distributed network encompassing fronto-parietal and parieto-temporal connections (Fig. 5A and Supplementary Table 6).

Analysis of the spatial distribution of nodes in this network showed different patterns of local-to-global connections in each group (Fig. 5B, Table 1 and Supplementary Table 5). Compared to controls, patients with bvFTD and frontal lesions presented reduced connections at medium and long-range distances (Fig. 5B). No differences were found among bvFTD and frontal lesions. Thus, fronto-temporo-parietal network connectivity associated with SOIS was affected in bvFTD and frontal lesions at medium and long-range distances.

The fronto-temporo-parietal association to SOIS was also observed when the network was estimated from controls only (Supplementary Fig. 4A) and then applied to all groups. Despite some differences, enhanced long-range connections were again observed in controls and Alzheimer's disease, when compared with frontal lesions and bvFTD (Supplementary material and Supplementary Fig. 4B). In addition, the comparison between groups exhibiting good (controls, Alzheimer's disease) and bad (bvFTD, frontal lesions) performance yielded significant differences with both networks (network estimated from all subjects and network estimated from controls subjects): middle/long-range connections were stronger in good performers (Supplementary Fig. 5).

Discussion

Successful everyday social interactions recursively incorporate own preferences with inferences about the other choices (Nicolle *et al.*, 2012; O'Callaghan *et al.*, 2016; Lee and Seo, 2016). By integrating self-interest values predictions about other-regarding preferences, decision makers adjust their behaviour and update social strategies to optimize social outcomes (Seo and Lee, 2012; Lee and Seo, 2016). In the current work we administrated a repeated version of the ultimatum game paradigm to investigate social bargaining behaviour in two neurodegenerative conditions (bvFTD and Alzheimer's disease) and unilateral frontal stroke. We used a multi-dimensional lesion approach to study three key processes of social bargaining strategy: two basic decision-making indexes reflecting self-interest choice and the adaptation to others' perspectives (ASP, AOP) and a more

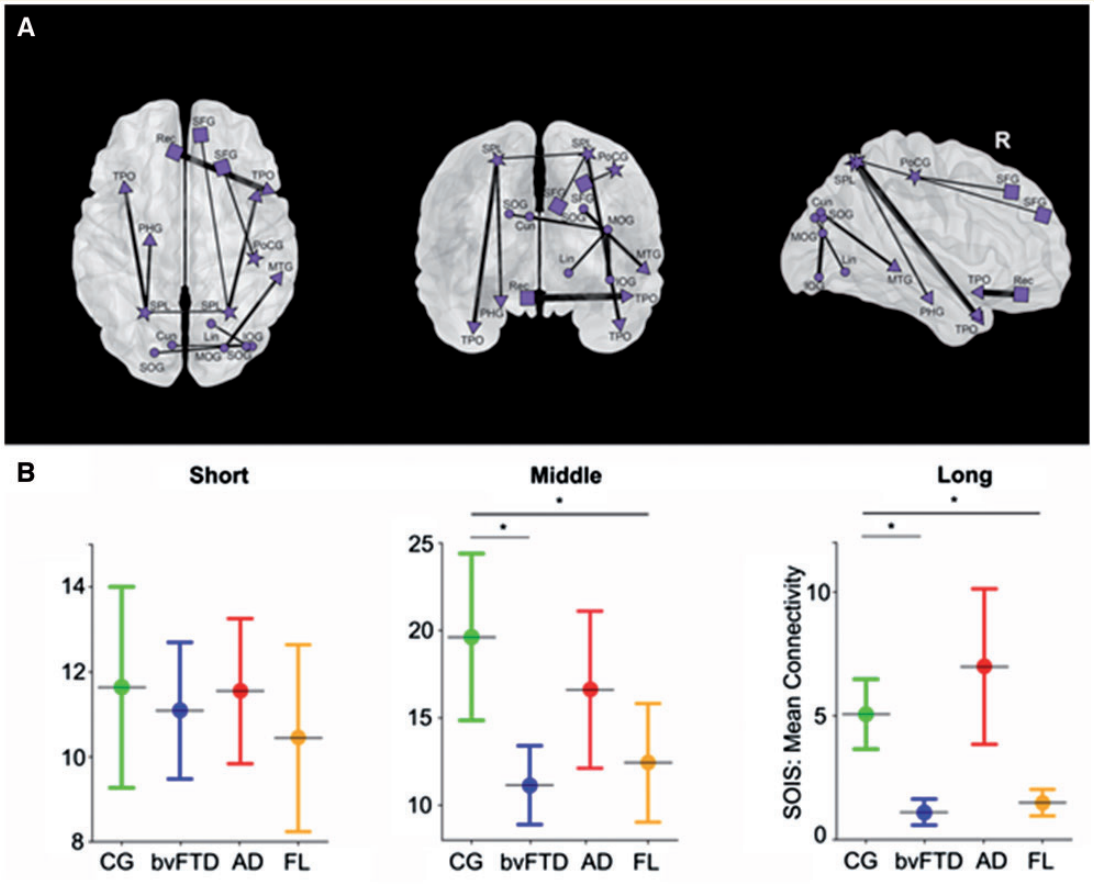

Figure 5 Functional connectivity. (**A**) Distributed network encompassing fronto-parieto-temporal connections revealed by the association between functional connectivity and the SOIS index across groups. (**B**) Different patterns of local-to-global connections in each group revealed by the analysis of the spatial distribution of nodes in this network. Reduced connections at medium and long-range distances in patients with bvFTD and frontal lesions compared to controls. No differences between bvFTD and frontal lesions were observed. Cun = cuneus; PHG = parahippocampal gyrus; IOG = inferior occipital gyrus; Lin = lingual gyrus; MOG = middle occipital gyrus; MTG = middle temporal gyrus; PoCG = postcentral gyrus; Rec = gyrus rectus; SFG = superior frontal gyrus; SOG = superior occipital gyrus; SPL = superior parietal lobule; TPO = temporal pole. CG = controls; AD = Alzheimer's disease; FL = frontal lesion.

complex integrative decision index (SOIS), critical for successful long-run strategy based on self-other perspectives integration. Specifically, the subtle and flexible adaptation to implicit changes in a negotiation setting critically depends on prefrontal networks and related changes in functional connectivity and oscillatory signatures. To our knowledge, this is the first study that combines behavioural, temporal–dynamic, and structural/functional brain signatures of social bargaining and provided convergent evidence of the critical roles of frontal hubs and its related temporal-parietal networks in the dynamic integration of social bargaining.

Behavioural results

Intact basic social bargaining measures (ASP, AOP) were observed in all clinical groups. Moreover, given that the simulation generates players with different thresholds of acceptance and rejection (Supplementary material), the responder's decisions were not fixed. However, they did not differ across controls and clinical groups (Supplementary material).

Previous research on poor individual decision-making in bvFTD (Rahman *et al.*, 1999; Gleichgerrcht *et al.*, 2010) has focused on specific aspects (probability, risk, ambiguity) of non-social decision-making. Also, in line with present results, bvFTD patients have been shown to perform similarly to controls in the basic ultimatum game (basic fairness performance playing as 'responders') (O'Callaghan *et al.*, 2016). On the other hand, results from the frontal lesions group align with evidence that ventromedial prefrontal cortex lesion patients have intact self-interest and fairness-based decisions alongside impairments in adaptation to long-term consequences (Moretti *et al.*, 2009). Finally, as regards Alzheimer's disease, evidence is mixed concerning decision-making (Torralva *et al.*, 2000; Sinz *et al.*, 2008) and null in terms of social bargaining. Our Alzheimer's disease group did not differ from

Table 1 Association between local-to-global connection and SOIS index

	Controls versus bvFTD		Controls versus Alzheimer's disease		Controls versus frontal lesions	
	P-value	T	*P*-value	T	*P*-value	T
Long	0.000	8.55	0.000	−3.62	0.000	7.30
Middle	0.000	7.02	0.059	1.97	0.000	5.12
Short	0.410	0.84	0.892	0.13	0.130	1.52

controls on any social bargaining measure, arguably to their relative frontal preservation (Kloeters *et al.*, 2013). Interestingly, the Alzheimer's disease group showed deficits in non-bargaining decisional measures (normative risk adjustment, consistency of the offer; Supplementary material). This might be related to the patients' parietal atrophy, given the role of parietal structures in outcome probability adjustments (Studer *et al.*, 2015). In brief, while patients with Alzheimer's disease exhibited inconsistent offers and impaired probability adjustment, they were able to deploy successful long-term social negotiation.

Crucially, patients with bvFTD and frontal lesions showed SOIS impairments relative to controls. Overall behavioural results suggest that strategic social decisions, based on constant updates and adjustments integrating self and others' preferences (Seo and Lee, 2012), depend critically on prefrontal networks and are partially independent from more basic decision-making skills. For more details on the social decision-making styles of the clinical groups and further discussion of which factors influence SOIS performance, see the online Supplementary material.

Brain structural correlates of social bargaining

Results provide multimodal unprecedented evidence for the crucial role of frontal areas in social strategic behaviour (SOIS), as discussed below. SOIS was directly related with preservation of frontal structures: in bvFTD, impaired performance was positively associated with reduced grey matter in the ventromedial prefrontal cortex (and extending to the left inferior/superior temporal gyrus), while in patients with frontal lesions these deficits were linked with lesions of the right superior, middle, and inferior frontal gyri. Similarly, in Alzheimer's disease, SOIS was predicted by the volume of left middle orbitofrontal cortex. Despite high individual variability in this strategy (Fig. 1), the Alzheimer's disease group exhibited preserved performance associated with (spared) prefrontal cortex. Similar results were obtained with additional masking analyses. Furthermore, we observed an additional involvement of the ventromedial prefrontal cortex in frontal lesions, thus revealing a specific convergence of this area in both frontal patient groups with affected social strategic behaviour. Nevertheless, note that this is a restrictive analysis, given that whole-brain results evince an association between SOIS scores and different portions of frontal structures.

These results shed light on two critical aspects of frontal structures. Despite the critical role of parietal, temporal, and insular regions in decision-making (Platt and Glimcher, 1999; Sanfey *et al.*, 2003; Krain *et al.*, 2006; Sanfey, 2007; Kiani and Shadlen, 2009; Studer *et al.*, 2015) and strategic thinking (Coricelli and Nagel, 2009; Bhatt *et al.*, 2010), our structural analysis revealed a predominance of prefrontal involvement in SOIS-related regions across clinical samples. This predominance corroborates the critical role of prefrontal regions for developing a successful strategy, even if other related processes associated to posterior regions are affected; for details on non-bargaining specific behavioural deficits in Alzheimer's disease, see Supplementary material, and Studer *et al.* (2015). Also, masking analyses showed additional involvement of the ventromedial prefrontal cortex in frontal lesions, highlighting this area as a specific convergence point in both frontal disorders with affected SOIS. Nevertheless, note that this is a restrictive analysis, given that whole-brain results evince an association between SOIS and different portions of frontal structures. Indeed, our findings suggest that similar processes underlying complex social decision-making involve different prefrontal structures. This is expected in light of previous evidence that high-level decision-making can be influenced by a variety of prefrontal hubs. Research on decision-making under ambiguity has shown that patients with discrete damage to both dorsolateral and dorsomedial prefrontal regions display similar impairments (Manes *et al.*, 2002). Also, several works have highlighted the critical role of both the orbitofrontal cortex and the anterior cingulate cortex in reinforcement-guided decision-making (for a review see Rushworth *et al.*, 2007). In addition, social context cues in social-norm-compliance tasks activate different portions of the prefrontal cortex, such as the dorsolateral, ventrolateral, and bilateral orbitofrontal structures (Spitzer *et al.*, 2007). All these findings suggest a multi-integrative role of prefrontal structures in social strategic behaviour.

In sum, convergent from our lesion models highlights the critical role of prefrontal regions to continuously adapt decisions to changing self-other perspectives. This finding aligns with evidence that bvFTD is characterized by difficulties to integrate social context information (Ibanez and Manes, 2012; Ibanez *et al.*, 2014*b*; Baez *et al.*, 2016*a*) and that prefrontal lesions involve aberrant long-term integration of social/non-social information during decision-making (Moretti *et al.*, 2009). Moreover, as discussed

below, this anatomo-clinical pattern was accompanied by altered frontotemporal oscillations and disturbed connectivity among extended functional networks.

Oscillatory correlates of social bargaining

As previously reported (Billeke *et al.*, 2013, 2014*a*, *b*, 2015), we found that risk behaviours associated with SOIS in controls involved oscillatory activity in the alpha/beta band (in right temporo-parietal and fronto-central scalp sites) between 800 and 1000 ms after the offer. Here, we extended this finding by showing that alpha/beta activity independently correlated with both ventromedial prefrontal cortex volume and SOIS performance. These findings confirm the essential role of frontal areas in key levels of social bargaining, from risk taking behaviour to the deployment of a successful long-term strategy. Recently, the ventromedial prefrontal cortex has been related with the integration of self-other preferences in altruistic non-interactive decisions (Hutcherson *et al.*, 2015). Moreover, source estimation revealed involvement of the medial prefrontal cortex, the temporo-parietal junction, and the inferior parietal lobe in modulating cognitive control (Dosenbach *et al.*, 2008) and social decision-making (Saxe, 2006; Zaki and Ochsner, 2009). Here, we confirmed that alpha/beta activity predicts risk of the proposer's offers, anticipates others' decisions (Billeke *et al.*, 2013), and predicts strategic long-term adaptations in social interactions (Billeke *et al.*, 2014*a*, 2015).

Nevertheless, such fronto-temporal activity did not predict SOIS and was reduced in clinical groups. This is expected given the frontal (bvFTD and frontal lesions) and posterior temporal (Alzheimer's disease) damage in these groups, and it may suggest that they have difficulties in evaluating the risk of their own offers while anticipating the others' most probable behaviours. By the same token, and despite the reservations imposed by our moderate sample size, present results revealed: (i) reduced frontotemporal activity in bvFTD relative to controls; (ii) reduced frontotemporal activity in frontal lesions, with significant differences in left temporo-parietal regions; and (iii) preserved early modulation in Alzheimer's disease in temporo-parietal regions, with a reduction observed only in late time windows (700–900 ms; for details of each group, see Supplementary material). These findings corroborate the essential role of frontal areas in SOIS and show that sensitive ongoing brain oscillations indexing anticipation of others' responses are selectively affected in the clinical groups, with greater deficits for bvFTD and frontal lesions than Alzheimer's disease.

Functional connectivity

Our findings of both SOIS networks (estimated with all groups or controls only) suggest that mid/long-range fronto-temporo-parietal connections predicted adequate social strategic behaviour. Moreover, analysis of global-to-local distances revealed that middle and long-range links of the SOIS network were selectively reduced in frontal disorders (bvFTD and frontal lesions). This network resembles those posited by fronto-temporo-parietal models indexing complex strategic decisions (Seo and Lee, 2012; Stallen and Sanfey, 2013; Ruff and Fehr, 2014; Lee and Seo, 2016). In sum, functional connectivity results suggest that strategic social bargaining relies not only on critical frontal hubs but also on long-range connections among hubs which span the entire social decision network.

In addition, these findings suggest that damage to critical frontal hubs affected their widespread connectivity to other relevant regions during the ongoing deployment of SOIS. Preserved social bargaining behaviour in Alzheimer's disease confirms this pattern (see also Chiong *et al.*, 2013), probably reflecting reduced medial prefrontal atrophy and more preserved distant connections. Spared long-distance connections in Alzheimer's disease can also be understood as a compensatory response to reduced temporal connectivity, as suggested by others (Buckner, 2004; Dickerson *et al.*, 2004; Gould *et al.*, 2006; Supekar *et al.*, 2008). Importantly, our results indicate that the ability to integrate both self-related and vicarious choices during social interaction goes beyond isolated loci and depends on large scale functional connectivity (Decety *et al.*, 2004; Hampton *et al.*, 2008; Hare *et al.*, 2010; Janowski *et al.*, 2013; Smith *et al.*, 2014). Similarly, these results confirm that signals from regions associated with social and non-social decisions are integrated within fronto-temporo-parietal networks (Cocchi *et al.*, 2013; Cole *et al.*, 2013; Janowski *et al.*, 2013). Complex social interaction strategies depend on switching among self and others' perspectives (Stallen and Sanfey, 2013), which also calls on large-scale brain networks (Cocchi *et al.*, 2013).

A convergent multilevel approach to strategic social negotiation

Difficulties in context-sensitive social adaptation is the hallmark of bvFTD and other frontal disorders (Baez *et al.*, 2012, 2016*a*; Ibanez and Manes, 2012; Baez and Ibanez, 2014). Neurodegeneration and stroke are two complementary lesion models that illuminate neuroanatomical correlates of such a pattern. Whereas the atrophy pattern in bvFTD often affects large-scale functional connections (Seeley *et al.*, 2009; Ibanez and Manes, 2012; Garcia-Cordero *et al.*, 2015), stable focal damage in stroke allows for functional compensation via plastic mechanisms (Rorden and Karnath, 2004; Grefkes and Fink, 2014). Despite these pathophysiological differences, both frontal lesion models showed similar structural, oscillatory, and functional connectivity abnormalities associated with impaired SOIS. Thus, this study offers robust multidimensional evidence of a critical role of prefrontal hubs in long-term social negotiation. In fact, this domain seems to

depend on the full integrity of a broad network cutting across anterior and posterior hubs, which can be similarly affected irrespective of the underlying physiopathology. This observation confirms the widely distributed and multi-dimensional nature of strategic social bargaining mechanisms.

Limitations and prospects for an emerging agenda

The ultimatum game engages other processes beyond the scope of this work. Specifically, social cognition calls on mentalizing and executive mechanisms (Decety *et al.*, 2004), which could be contemplated in additional research. Also, future studies of social bargaining assessing neuroimaging and/or electrophysiological correlates should include measures of individual differences in social cognition, emotions, and executive functions. Related to this last domain, in the present work, executive functions were affected in all clinical groups (Supplementary material) raising the possibility of primary executive dysfunction affecting the results. However, the choices among different possible offers require similar demand of executive function effort. Also, we did not find any group significant difference in basic bargaining performance (ASP, AOP). Moreover, we calculated the association between executive performance and the performance in the three indexes from all and each group, and found no single association (Supplementary material). Nevertheless, further task including conditions with dissimilar executive demands should assess the contribution of executive function in social negotiation.

Our sample size was moderate due to the difficulties inherent EEG and functional MRI in patient population. However, others studies yielded robust findings with similar or smaller sample sizes (Moretti *et al.*, 2009; Hughes *et al.*, 2011; Day *et al.*, 2013; Garcia-Cordero *et al.*, 2015). Also, our neuroanatomical findings were not obtained through an active functional MRI task. Yet, note that this would require a longer scanning session, which increases the risks of producing faulty data due to patients' movements. Although a few studies have obtained task-related functional MRI recordings (Chiong *et al.*, 2013), correlations between structural MRI and behavioural performance constitute the standard approach in the field (Mendez and Shapira, 2009; Chiong *et al.*, 2013; O'Callaghan *et al.*, 2016). In addition, we assessed ongoing oscillatory EEG correlates during the task to reduce the time of scanning sessions and complement our anatomical findings with dynamic neural data. However, future studies should extend present results by assessing direct functional MRI correlates.

The lack of data from neuropsychiatric questionnaires is another caveat of this study, as they provide useful information about behavioural changes. Future studies should assess the relations between neuropsychiatric and behavioural symptoms of Alzheimer's disease and bvFTD and the neurocognitive correlates of long-term strategic social decisions. This may illuminate the impact of specific physiopathological processes to on social bargaining behaviour.

Given that all clinical groups showed preserved basic bargaining performance, results from bvFTD and frontal lesions patients point to a specific and selective deficit in strategic long-term social reasoning. Our study opens a new agenda by extending previous findings of impaired strategic abilities, while showing for the first time that social long-term strategic negotiation is similarly affected in two frontal lesions models, irrespective of the underlying physiopathology. Yet, given the patients' limited attention span, we did not include an additional non-social condition, which makes it difficult to establish whether the observed deficits are specific to long-term social bargaining or a consequence of more general impairments in long-term planning. Future studies including both social and non-social aspects of long-term strategies are necessary to extend the findings we presented here

Strategic decision-making plays a crucial role in daily life, from specific interactions with other persons to financial decisions (Rilling *et al.*, 2004). Patients with frontal disorder presented impaired real world social functioning, with impulsive shopping, extravagant spending, and pathological gambling in both everyday life and experimental setting (Bechara, 2005; Manes *et al.*, 2011; O'Callaghan *et al.*, 2016). Future studies will be able to investigate if deficits in social bargaining predict the real life financial and social negotiation in these patients.

Finally, the functional connectivity association with SOIS revealed an additional association with occipital hubs. Future studies excluding visual modality or comparing visual as auditory task would explore whether this posterior activation reflects expected visual task-related demands or it is due to other cognitive process.

Conclusion

To summarize, the lesion model approach reveals critical links between affected brain regions and behavioural performance (Rorden and Karnath, 2004). The predominance of prefrontal involvement in SOIS-related regions across clinical samples indicates that frontal structures are critical for long-term social bargaining in comparison with other insular, temporal or posterior structures. Complementary multidimensional findings further suggest that strategic reasoning in social decision-making calls on complex neurocognitive mechanisms (Griessinger and Coricelli, 2015), and that the disruption of any of them can compromise the normal deployment of such skill. The variability in the specific prefrontal structures recruited by each group, together with the involvement of other (i) frontotemporal regions associated with ongoing oscillations; and (ii) fronto-temporo-parietal functional networks, emphasize the need

to identify the contribution of large-scale network interactions. To our knowledge, this is the first study to investigate strategic social bargaining in three lesion models. By combining structural, electrophysiological, and functional analysis with a simple but realistic negotiation task, we have shown that flexible and strategic adaptation to self-other preferences during bargaining depends critically on prefrontal hubs and related temporo-parietal networks.

The omission of dynamic interpersonal strategies in classical game theories probably lies at the heart of their failure to adequately predict everyday social decision-making (Seo and Lee, 2012; Stallen and Sanfey, 2013; Ruff and Fehr, 2014; Lee and Seo, 2016). Futures studies of behavioural economics should incorporate insights from cognitive neuroscience to provide more ecological predictive models of strategic social bargaining. In this sense, our results open novel pathways to understand how social bargaining mechanisms are functionally organized across cortical and subcortical regions, and how they can be specifically disrupted by varied forms of brain damage.

Funding

This work was partially supported by grants from CONICET, CONICYT/FONDECY T Regular (1130920, 1140423 and 1140114), COLCIENCIAS (1115-545-31374, contract: 392), FONCyT-PICT 2012-0412, FONCyT-PICT 2012-1309, CONICYT/FONDAP/15150012 and Associative Research Program of CONICYT under Grant Basal Funds for Centers of Excellence FB 0003 and the INECO Foundation.

Supplementary material

Supplementary material is available at *Brain* online.

References

Almairac F, Herbet G, Moritz-Gasser S, de Champfleur NM, Duffau H. The left inferior fronto-occipital fasciculus subserves language semantics: a multilevel lesion study. Brain Struct Funct 2015; 220: 1983–95.

Ashburner J, Friston KJ. Voxel-based morphometry—the methods. Neuroimage 2000; 11 (6 Pt 1): 805–21.

Baez S, Couto B, Torralva T, Sposato LA, Huepe D, Montanes P, et al. Comparing moral judgments of patients with frontotemporal dementia and frontal stroke. JAMA Neurol 2014a; 71: 1172–6.

Baez S, Garcia AM, Ibanez A. The social context network model in psychiatric and neurological diseases. Curr Top Behav Neurosci 2016a.

Baez S, Ibanez A. The effects of context processing on social cognition impairments in adults with Asperger's syndrome. Front Neurosci 2014; 8: 270.

Baez S, Kanske P, Matallana D, Montañes P, Reyes P, Slachevsky A, et al. Integration of intention and outcome for moral judgment in frontotemporal dementia: brain structural signatures. Neurodegener Dis 2016b; 16: 206–17.

Baez S, Manes F, Huepe D, Torralva T, Fiorentino N, Richter F, et al. Primary empathy deficits in frontotemporal dementia. Front Aging Neurosci 2014b; 6: 262.

Baez S, Morales JP, Slachevsky A, Torralva T, Matus C, Manes F, et al. Orbitofrontal and limbic signatures of empathic concern and intentional harm in the behavioral variant frontotemporal dementia. Cortex 2016c; 75: 20–32.

Baez S, Rattazzi A, Gonzalez-Gadea ML, Torralva T, Vigliecca NS, Decety J, et al. Integrating intention and context: assessing social cognition in adults with Asperger syndrome. Front Hum Neurosci 2012; 6: 302.

Baillet S, Mosher J, Leahy R. Electromagnetic brain mapping. IEEE Signal Process Mag 2001; 18: 14–30.

Bates E, Wilson SM, Saygin AP, Dick F, Sereno MI, Knight RT, et al. Voxel-based lesion-symptom mapping. Nat Neurosci 2003; 6: 448–50.

Bechara A. Decision-making, impulse control and loss of willpower to resist drugs: a neurocognitive perspective. Nat Neurosci 2005; 8: 1458–63.

Behrens TE, Hunt LT, Rushworth MF. The computation of social behavior. Science 2009; 324: 1160–4.

Benjamini Y, Hochberg Y. Controlling the false discovery rate: a practical and powerful approach to multiple testing. J R Stat Soc 1995; 57: 289–300.

Bhatt MA, Lohrenz T, Camerer CF, Montague PR. Neural signatures of strategic types in a two-person bargaining game. Proc Natl Acad Sci USA 2010; 107: 19720–5.

Billeke P, Armijo A, Castillo D, Lopez T, Zamorano F, Cosmelli D, et al. Paradoxical expectation: oscillatory brain activity reveals social interaction impairment in schizophrenia. Biol Psychiatry 2015; 78: 421–31.

Billeke P, Zamorano F, Chavez M, Cosmelli D, Aboitiz F. Functional cortical network in alpha band correlates with social bargaining. PLoS One 2014a; 9: e109829.

Billeke P, Zamorano F, Cosmelli D, Aboitiz F. Oscillatory brain activity correlates with risk perception and predicts social decisions. Cereb Cortex 2013; 23: 2872–83.

Billeke P, Zamorano F, Lopez T, Rodriguez C, Cosmelli D, Aboitiz F. Someone has to give in: theta oscillations correlate with adaptive behavior in social bargaining. Soc Cogn Affect Neurosci 2014b; 9: 2041–8.

Bonthius DJ, Solodkin A, Van Hoesen GW. Pathology of the insular cortex in Alzheimer disease depends on cortical architecture. J Neuropathol Exp Neurol 2005; 64: 910–22.

Braak H, Braak E. Neuropathological stageing of Alzheimer-related changes. Acta Neuropathol 1991; 82: 239–59.

Brand M, Labudda K, Markowitsch HJ. Neuropsychological correlates of decision-making in ambiguous and risky situations. Neural Netw 2006; 19: 1266–76.

Brunner E, Munzel U. The nonparametric behrens-fisher problem: asymptotic theory and a small-sample approximation. Biom J 2000; 42: 17–25.

Bruno JL, Garrett AS, Quintin EM, Mazaika PK, Reiss AL. Aberrant face and gaze habituation in fragile x syndrome. Am J Psychiatry 2014; 171: 1099–106.

Buckner RL. Memory and executive function in aging and AD: multiple factors that cause decline and reserve factors that compensate. Neuron 2004; 44: 195–208.

Burgess PW, Shallice T. Response suppression, initiation and strategy use following frontal lobe lesions. Neuropsychologia 1996; 34: 263–72.

Chiong W, Wilson SM, D'Esposito M, Kayser AS, Grossman SN, Poorzand P, et al. The salience network causally influences default mode network activity during moral reasoning. Brain 2013; 136 (Pt 6): 1929–41.

Clark L, Manes F, Antoun N, Sahakian BJ, Robbins TW. The contributions of lesion laterality and lesion volume to decision-making

impairment following frontal lobe damage. Neuropsychologia 2003; 41: 1474–83.
Cocchi L, Zalesky A, Fornito A, Mattingley JB. Dynamic cooperation and competition between brain systems during cognitive control. Trends Cogn Sci 2013; 17: 493–501.
Cole MW, Reynolds JR, Power JD, Repovs G, Anticevic A, Braver TS. Multi-task connectivity reveals flexible hubs for adaptive task control. Nat Neurosci 2013; 16: 1348–55.
Coricelli G, Nagel R. Neural correlates of depth of strategic reasoning in medial prefrontal cortex. Proc Natl Acad Sci USA 2009; 106: 9163–8.
Couto B, Manes F, Montanes P, Matallana D, Reyes P, Velasquez M, et al. Structural neuroimaging of social cognition in progressive non-fluent aphasia and behavioral variant of frontotemporal dementia. Front Hum Neurosci 2013; 7: 467.
Cristofori I, Moretti L, Harquel S, Posada A, Deiana G, Isnard J, et al. Theta signal as the neural signature of social exclusion. Cereb Cortex 2013; 23: 2437–47.
Cummings JL, Cole G. Alzheimer disease. JAMA 2002; 287: 2335–8.
Day GS, Farb NA, Tang-Wai DF, Masellis M, Black SE, Freedman M, et al. Salience network resting-state activity: prediction of frontotemporal dementia progression. JAMA Neurol 2013; 70: 1249–53.
Decety J, Jackson PL, Sommerville JA, Chaminade T, Meltzoff AN. The neural bases of cooperation and competition: an fMRI investigation. Neuroimage 2004; 23: 744–51.
Delgado MR, Frank RH, Phelps EA. Perceptions of moral character modulate the neural systems of reward during the trust game. Nat Neurosci 2005; 8: 1611–18.
Devor A, Bandettini PA, Boas DA, Bower JM, Buxton RB, Cohen LB, et al. The challenge of connecting the dots in the B.R.A.I.N. Neuron 2013; 80: 270–4.
Dickerson BC, Salat DH, Bates JF, Atiya M, Killiany RJ, Greve DN, et al. Medial temporal lobe function and structure in mild cognitive impairment. Ann Neurol 2004; 56: 27–35.
Donoso M, Collins AG, Koechlin E. Human cognition. Foundations of human reasoning in the prefrontal cortex. Science 2014; 344: 1481–6.
Dosenbach NU, Fair DA, Cohen AL, Schlaggar BL, Petersen SE. A dual-networks architecture of top-down control. Trends Cogn Sci 2008; 12: 99–105.
Du AT, Schuff N, Kramer JH, Rosen HJ, Gorno-Tempini ML, Rankin K, et al. Different regional patterns of cortical thinning in Alzheimer's disease and frontotemporal dementia. Brain 2007; 130 (Pt 4): 1159–66.
Ernst M, Bolla K, Mouratidis M, Contoreggi C, Matochik JA, Kurian V, et al. Decision-making in a risk-taking task: a PET study. Neuropsychopharmacology 2002; 26: 682–91.
Falquez R, Couto B, Ibanez A, Freitag MT, Berger M, Arens EA, et al. Detaching from the negative by reappraisal: the role of right superior frontal gyrus (BA9/32). Front Behav Neurosci 2014; 8: 165.
Ferreira LK, Diniz BS, Forlenza OV, Busatto GF, Zanetti MV. Neurostructural predictors of Alzheimer's disease: a meta-analysis of VBM studies. Neurobiol Aging 2011; 32: 1733–41.
Folstein MF, Robins LN, Helzer JE. The mini-mental state examination. Arch Gen Psychiatry 1983; 40: 812.
Garcia-Cordero I, Sedeno L, Fraiman D, Craiem D, de la Fuente LA, Salamone P, et al. Stroke and neurodegeneration induce different connectivity aberrations in the insula. Stroke 2015; 46: 2673–7.
García-Cordero I, Sedeño L, de la Fuente L, Slachevsky A, Forno G, Klein F, et al. Feeling, learning from, and being aware of inner states: interoceptive dimensions in neurodegeneration and stroke. Phil Trans R Soc B 2016. doi: 10.1098/rstb.2016-0006, in press.
Gleichgerrcht E, Ibanez A, Roca M, Torralva T, Manes F. Decision-making cognition in neurodegenerative diseases. Nat Rev Neurol 2010; 6: 611–23.
Gonzalez-Gadea ML, Chennu S, Bekinschtein TA, Rattazzi A, Beraudi A, Tripicchio P, et al. Predictive coding in autism spectrum disorder and attention deficit hyperactivity disorder. J Neurophysiol 2015; 114: 2625–36.
Good CD, Johnsrude IS, Ashburner J, Henson RN, Friston KJ, Frackowiak RS. A voxel-based morphometric study of ageing in 465 normal adult human brains. Neuroimage 2001; 14 (1 Pt 1): 21–36.
Gould RL, Arroyo B, Brown RG, Owen AM, Bullmore ET, Howard RJ. Brain mechanisms of successful compensation during learning in Alzheimer disease. Neurology 2006; 67: 1011–17.
Grefkes C, Fink GR. Connectivity-based approaches in stroke and recovery of function. Lancet Neurol 2014; 13: 206–16.
Griessinger T, Coricelli G. The neuroeconomics of strategic interaction. Curr Opin Behav Sci 2015; 3: 73–9.
Hampton AN, Bossaerts P, O'Doherty JP. Neural correlates of mentalizing-related computations during strategic interactions in humans. Proc Natl Acad Sci USA 2008; 105: 6741–6.
Han Z, Bi Y, Chen J, Chen Q, He Y, Caramazza A. Distinct regions of right temporal cortex are associated with biological and human-agent motion: functional magnetic resonance imaging and neuropsychological evidence. J Neurosci 2013; 33: 15442–53.
Hare TA, Camerer CF, Knoepfle DT, Rangel A. Value computations in ventral medial prefrontal cortex during charitable decision-making incorporate input from regions involved in social cognition. J Neurosci 2010; 30: 583–90.
Henseler I, Regenbrecht F, Obrig H. Lesion correlates of patholinguistic profiles in chronic aphasia: comparisons of syndrome-, modality- and symptom-level assessment. Brain 2014; 137 (Pt 3): 918–30.
Hesse E, Mikulan E, Decety J, Sigman M, Garcia Mdel C, Silva W, et al. Early detection of intentional harm in the human amygdala. Brain 2016; 139 (Pt 1): 54–61.
Hughes LE, Nestor PJ, Hodges JR, Rowe JB. Magnetoencephalography of frontotemporal dementia: spatiotemporally localized changes during semantic decisions. Brain 2011; 134 (Pt 9): 2513–22.
Hutcherson CA, Bushong B, Rangel A. A neurocomputational model of altruistic choice and its implications. Neuron 2015; 87: 451–62.
Ibanez A, Aguado J, Baez S, Huepe D, Lopez V, Ortega R, et al. From neural signatures of emotional modulation to social cognition: individual differences in healthy volunteers and psychiatric participants. Social Cogn Affect Neurosci 2014a; 9: 939–50.
Ibanez A, Kuljis RO, Matallana D, Manes F. Bridging psychiatry and neurology through social neuroscience. World Psychiatry 2014b; 13: 148–9.
Ibanez A, Manes F. Contextual social cognition and the behavioral variant of frontotemporal dementia. Neurology 2012; 78: 1354–62.
Ibanez A, Melloni M, Huepe D, Helgiu E, Rivera-Rei A, Canales-Johnson A, et al. What event-related potentials (ERPs) bring to social neuroscience? Soc Neurosci 2012; 7: 632–49.
Irish M, Hodges JR, Piguet O. Right anterior temporal lobe dysfunction underlies theory of mind impairments in semantic dementia. Brain 2014a; 137 (Pt 4): 1241–53.
Irish M, Piguet O, Hodges JR, Hornberger M. Common and unique gray matter correlates of episodic memory dysfunction in frontotemporal dementia and Alzheimer's disease. Hum Brain Mapp 2014b; 35: 1422–35.
Janowski V, Camerer C, Rangel A. Empathic choice involves vmPFC value signals that are modulated by social processing implemented in IPL. Soc Cogn Affect Neurosci 2013; 8: 201–8.
Kable JW, Glimcher PW. The neurobiology of decision: consensus and controversy. Neuron 2009; 63: 733–45.
Kiani R, Shadlen MN. Representation of confidence associated with a decision by neurons in the parietal cortex. Science 2009; 324: 759–64.
Kipps CM, Nestor PJ, Acosta-Cabronero J, Arnold R, Hodges JR. Understanding social dysfunction in the behavioural variant of frontotemporal dementia: the role of emotion and sarcasm processing. Brain 2009; 132 (Pt 3): 592–603.
Kishida KT, King-Casas B, Montague PR. Neuroeconomic approaches to mental disorders. Neuron 2010; 67: 543–54.

Kloeters S, Bertoux M, O'Callaghan C, Hodges JR, Hornberger M. Money for nothing - Atrophy correlates of gambling decision-making in behavioural variant frontotemporal dementia and Alzheimer's disease. Neuroimage Clin 2013; 2: 263–72.
Koenigs M, Tranel D. Irrational economic decision-making after ventromedial prefrontal damage: evidence from the Ultimatum Game. J Neurosci 2007; 27: 951–6.
Krain AL, Wilson AM, Arbuckle R, Castellanos FX, Milham MP. Distinct neural mechanisms of risk and ambiguity: a meta-analysis of decision-making. Neuroimage 2006; 32: 477–84.
Krajbich I, Adolphs R, Tranel D, Denburg NL, Camerer CF. Economic games quantify diminished sense of guilt in patients with damage to the prefrontal cortex. J Neurosci 2009; 29: 2188–92.
Lambon Ralph MA, Cipolotti L, Manes F, Patterson K. Taking both sides: do unilateral anterior temporal lobe lesions disrupt semantic memory? Brain 2010; 133: 3243–55.
Lee D. Game theory and neural basis of social decision-making. Nat Neurosci 2008; 11: 404–9.
Lee D, Seo H. Neural Basis of Strategic Decision-making. Trends Neurosci 2016; 39: 40–8.
Lerch JP, Pruessner JC, Zijdenbos A, Hampel H, Teipel SJ, Evans AC. Focal decline of cortical thickness in Alzheimer's disease identified by computational neuroanatomy. Cereb Cortex 2005; 15: 995–1001.
Manes F, Sahakian B, Clark L, Rogers R, Antoun N, Aitken M, et al. Decision-making processes following damage to the prefrontal cortex. Brain 2002; 125 (Pt 3): 624–39.
Manes F, Torralva T, Ibanez A, Roca M, Bekinschtein T, Gleichgerrcht E. Decision-making in frontotemporal dementia: clinical, theoretical and legal implications. Dement Geriatr Cogn Disord 2011; 32: 11–7.
Maris E, Oostenveld R. Nonparametric statistical testing of EEG- and MEG-data. J Neurosci Methods 2007; 164: 177–90.
Mazaika PK, Hoeft F, Glover GH, Reiss, AL. Methods and software for fMRI analysis for clinical subjects. Hum Brain Mapp 2009; 33: 609–27.
McKhann G, Drachman D, Folstein M, Katzman R, Price D, Stadlan EM. Clinical diagnosis of Alzheimer's disease: report of the NINCDS-ADRDA Work Group under the auspices of Department of Health and Human Services Task Force on Alzheimer's Disease. Neurology 1984; 34: 939–44.
McKhann GM, Knopman DS, Chertkow H, Hyman BT, Jack CR Jr., Kawas CH, et al. The diagnosis of dementia due to Alzheimer's disease: recommendations from the National Institute on Aging-Alzheimer's Association workgroups on diagnostic guidelines for Alzheimer's disease. Alzheimers Dement 2011; 7: 263–9.
Melloni M, Sedeño L, Hesse E, García-Cordero I, Mikulan E, Plastino A, et al. Cortical dynamics and subcortical signatures of motor-language coupling in Parkinson's disease. Sci Rep 2015; 5: 11899.
Mendez MF, Shapira JS. Altered emotional morality in frontotemporal dementia. Cogn Neuropsychiatry 2009; 14: 165–79.
Mioshi E, Dawson K, Mitchell J, Arnold R, Hodges JR. The Addenbrooke's Cognitive Examination Revised (ACE-R): a brief cognitive test battery for dementia screening. Int J Geriatr Psychiatry 2006; 21: 1078–85.
Moretti L, Dragone D, di Pellegrino G. Reward and social valuation deficits following ventromedial prefrontal damage. J Cogn Neurosci 2009; 21: 128–40.
Naggara O, Oppenheim C, Rieu D, Raoux N, Rodrigo S, Dalla Barba G, et al. Diffusion tensor imaging in early Alzheimer's disease. Psychiatry Res 2006; 146: 243–9.
Neary D, Snowden JS, Gustafson L, Passant U, Stuss D, Black S, et al. Frontotemporal lobar degeneration: a consensus on clinical diagnostic criteria. Neurology 1998; 51: 1546–54.
Nichols TE, Holmes AP. Nonparametric permutation tests for functional neuroimaging: a primer with examples. Hum Brain Mapp 2002; 15: 1–25.
Nicolle A, Klein-Flugge MC, Hunt LT, Vlaev I, Dolan RJ, Behrens TE. An agent independent axis for executed and modeled choice in medial prefrontal cortex. Neuron 2012; 75: 1114–21.
O'Callaghan C, Bertoux M, Irish M, Shine JM, Wong S, Spiliopoulos L, et al. Fair play: social norm compliance failures in behavioural variant frontotemporal dementia. Brain 2016; 139 (Pt 1): 204–16.
Piguet O, Hornberger M, Mioshi E, Hodges JR. Behavioural-variant frontotemporal dementia: diagnosis, clinical staging, and management. Lancet Neurol 2011; 10: 162–72.
Platt ML, Glimcher PW. Neural correlates of decision variables in parietal cortex. Nature 1999; 400: 233–8.
Rahman S, Sahakian BJ, Hodges JR, Rogers RD, Robbins TW. Specific cognitive deficits in mild frontal variant frontotemporal dementia. Brain 1999; 122 (Pt 8): 1469–93.
Rascovsky K, Hodges JR, Kipps CM, Johnson JK, Seeley WW, Mendez MF, et al. Diagnostic criteria for the behavioral variant of frontotemporal dementia (bvFTD): current limitations and future directions. Alzheimer Dis Assoc Disord 2007; 21: S14–18.
Rascovsky K, Hodges JR, Knopman D, Mendez MF, Kramer JH, Neuhaus J, et al. Sensitivity of revised diagnostic criteria for the behavioural variant of frontotemporal dementia. Brain 2011; 134 (Pt 9): 2456–77.
Ratnavalli E, Brayne C, Dawson K, Hodges JR. The prevalence of frontotemporal dementia. Neurology 2002; 58: 1615–21.
Rilling JK, Sanfey AG, Aronson JA, Nystrom LE, Cohen JD. The neural correlates of theory of mind within interpersonal interactions. Neuroimage 2004; 22: 1694–703.
Rorden C, Karnath HO. Using human brain lesions to infer function: a relic from a past era in the fMRI age? Nat Rev Neurosci 2004; 5: 813–9.
Rorden C, Karnath HO, Bonilha L. Improving lesion-symptom mapping. J Cogn Neurosci 2007; 19: 1081–8.
Rosen HJ, Gorno-Tempini ML, Goldman WP, Perry RJ, Schuff N, Weiner M, et al. Patterns of brain atrophy in frontotemporal dementia and semantic dementia. Neurology 2002; 58: 198–208.
Rubinov M, Sporns O. Complex network measures of brain connectivity: uses and interpretations. Neuroimage 2010; 52: 1059–69.
Ruff CC, Fehr E. The neurobiology of rewards and values in social decision-making. Nat Rev Neurosci 2014; 15: 549–62.
Rushworth MF, Behrens TE, Rudebeck PH, Walton ME. Contrasting roles for cingulate and orbitofrontal cortex in decisions and social behaviour. Trends Cogn Sci 2007; 11: 168–76.
Sanfey AG. Social decision-making: insights from game theory and neuroscience. Science 2007; 318: 598–602.
Sanfey AG, Rilling JK, Aronson JA, Nystrom LE, Cohen JD. The neural basis of economic decision-making in the Ultimatum game. Science 2003; 300: 1755–8.
Saxe R. Uniquely human social cognition. Curr Opin Neurobiol 2006; 16: 235–9.
Sedeño L, Couto B, García Cordero I, Melloni M, Baez S, Morales J, et al. Network centrality in regions of early atrophy in frontotemporal dementia and social executive performance. J Int Neuropsychol Soc 2015: 250– 62.
Seeley WW, Crawford RK, Zhou J, Miller BL, Greicius MD. Neurodegenerative diseases target large-scale human brain networks. Neuron 2009; 62: 42–52.
Seo H, Lee D. Neural basis of learning and preference during social decision-making. Curr Opin Neurobiol 2012; 22: 990–5.
Sharp C, Monterosso J, Montague PR. Neuroeconomics: a bridge for translational research. Biol Psychiatry 2012; 72: 87–92.
Sinz H, Zamarian L, Benke T, Wenning GK, Delazer M. Impact of ambiguity and risk on decision-making in mild Alzheimer's disease. Neuropsychologia 2008; 46: 2043–55.
Smith DV, Clithero JA, Boltuck SE, Huettel SA. Functional connectivity with ventromedial prefrontal cortex reflects subjective value for social rewards. Soc Cogn Affect Neurosci 2014; 9: 2017–25.

Sollberger M, Stanley CM, Wilson SM, Gyurak A, Beckman V, Growdon M, et al. Neural basis of interpersonal traits in neurodegenerative diseases. Neuropsychologia 2009; 47: 2812–27.

Spitzer M, Fischbacher U, Herrnberger B, Gron G, Fehr E. The neural signature of social norm compliance. Neuron 2007; 56: 185–96.

Sporns O. Structure and function of complex brain networks. Dialogues Clin Neurosci 2013; 15: 247–62.

Stallen M, Sanfey AG. The cooperative brain. Neuroscientist 2013; 19: 292–303.

Stone VE, Cosmides L, Tooby J, Kroll N, Knight RT. Selective impairment of reasoning about social exchange in a patient with bilateral limbic system damage. Proc Natl Acad Sci USA 2002; 99: 11531–6.

Studer B, Manes F, Humphreys G, Robbins TW, Clark L. Risk-sensitive decision-making in patients with posterior parietal and ventromedial prefrontal cortex injury. Cereb Cortex 2015; 25: 1–9.

Supekar K, Menon V, Rubin D, Musen M, Greicius MD. Network analysis of intrinsic functional brain connectivity in Alzheimer's disease. PLoS Comput Biol 2008; 4: e1000100.

Torralva T, Dorrego F, Sabe L, Chemerinski E, Starkstein SE. Impairments of social cognition and decision-making in Alzheimer's disease. Int Psychogeriatr 2000; 12: 359–68.

Torralva T, Roca M, Gleichgerrcht E, Lopez P, Manes F. INECO Frontal Screening (IFS): a brief, sensitive, and specific tool to assess executive functions in dementia. J Int Neuropsychol Soc 2009; 15: 777–86.

Tzourio-Mazoyer N, Landeau B, Papathanassiou D, Crivello F, Etard O, Delcroix N, et al. Automated anatomical labeling of activations in SPM using a macroscopic anatomical parcellation of the MNI MRI single-subject brain. Neuroimage 2002; 15: 273–89.

Vickery TJ, Chun MM, Lee D. Ubiquity and specificity of reinforcement signals throughout the human brain. Neuron 2011; 72: 166–77.

Whitwell JL, Przybelski SA, Weigand SD, Ivnik RJ, Vemuri P, Gunter JL, et al. Distinct anatomical subtypes of the behavioural variant of frontotemporal dementia: a cluster analysis study. Brain 2009; 132 (Pt 11): 2932–46.

Zaki J, Mitchell JP. Equitable decision-making is associated with neural markers of intrinsic value. Proc Natl Acad Sci USA 2011; 108: 19761–6.

Zaki J, Ochsner K. The need for a cognitive neuroscience of naturalistic social cognition. Ann N Y Acad Sci 2009; 1167: 16–30.

SUPPLEMENTARY DATA

1. Material and methods

1.1. Participants

As in previous reports by our group (Torralva *et al.*, 2009a; Torralva *et al.*, 2009b; Gleichgerrcht *et al.*, 2011; Baez *et al.*, 2014; Garcia-Cordero *et al.*, 2015), diagnosis was initially made by a group of experts in dementia. Data from each patient was reviewed, individually, in the context of a multidisciplinary clinical meeting involving cognitive neurologists, psychiatrists, and neuropsychologists. Dementia patients were recruited as part of a broader ongoing study. BvFTD patients were included only if they showed frontal or temporal atrophy on MRI. All patients were in early/mild stages of the disease and did not meet criteria for specific psychiatric disorders, as assessed by psychiatric examination. Patients presenting primarily with language deficits were excluded. In patients with chronic cerebrovascular lesions (FL), damage was confined to frontal and insular structures. They also presented secondary damage in the putamen, the temporal poles, and frontal and parietal regions. Their diagnoses were made by stroke specialists. FL patients did not present with acute and transient symptomatology or residual signs at neurological examination, despite subtle complaints of subjective changes in some cases. In all cases, structural magnetic resonance imaging (MRI) of the brain, scanned between 6 and 12 months after the stroke, showed ischemic focal lesions, and none of them presented aphasia. All patients were able to complete general neuropsychological tests.

Finally, control subjects were matched one by one with any of the patients. Matching criteria were sex, age (± 4 years), and years of education (± 4 years). Control subjects were recruited via a database of healthy volunteers who did not have a history of drug abuse or a family history of neurodegenerative or psychiatric disorders. They were all part of an ongoing project.

1.2 Social bargaining: behavioral task

Regarding the acceptance rate, the simulation generates various virtual players, with different thresholds to accept or reject the offer. In other words, a lower offer can be

accepted by one virtual player but rejected by other. The rationale behind this point is that normal performance requires subjects to adapt their decisions while integrating the partner's specific preference within each game. This also ensures that the most subjects receive face both acceptances and rejection. Moreover, although the probability of acceptance varies among simulated responders, the mean of the probability of acceptance for the two most frequent offers are as follows (expressed as the money the proposer proposes to keep):

Money for the Proposer	Probability of Acceptance	Expected Reward
$ 50	0.86 (0.8-0.9)	43 (40 - 45)
$ 60	0.71 (0.65 0.76)	42.6 (39.6 – 45.6)

The variation among subjects and simulated responders implies that these two strategies did not differ in the optimization of the final earnings. Since the change of the strategy between human and computer games occurs in this range for most of the subjects, the behavioral change was guided by the proposer's belief concerning the responder's behavior rather than by a rational, maximized strategy or reinforcement learning alone.

1.3. Non-specific social bargaining measures: Behavioral study task

1.3.1. Normative risk adjustment (NRA): We computed the mean of the first offer per subject in each game. As in the first offer the subject did not have any information regarding the peer's preferences, this index refers mainly the adjusted general probability of winning/losing.

1.3.2. Consistency of the offers (CO): We computed the mean of the standard deviation of the offer through each game. This index reflects how subjects present fluctuation's behavior during the game.

1.4. Self-other integration strategy (SOIS)

Schematic representation of the SOIS calculation:

Logit $_{\textbf{g(game number) r(round number)}}$

	Round 1	Round 2	…	Round 20
Game 1	Logit $_{g = 1 r = 1}$	Logit $_{g = 1 r = 2}$	…	Logit $_{g = 1 r = 20}$
Game 2	Logit $_{g = 2 r = 1}$			
…	…			
Game 8	Logit $_{g = 8 r = 1}$	Logit $_{g = 1 r = 2}$	…	Logit $_{g = 8 r = 20}$
Mean		**Logit** $_{\textbf{g = mean r = 2}}$	**…**	**Logit** $_{\textbf{g = mean r = 20}}$

Columns represent the round of each game, and rows represent each game. For each round (range between 2 to 20), we averaged the mean of the logit across all of the eight games. Both logit and round number were rank-transformed to obtain Spearman's correlations. By deriving SOIS scores this way, we minimized the influence of the AOP and ASP indexes in its computation.

1.5. Electroencephalographic recordings

Electroencephalographic (EEG) signals were recorded online while participants performed the UG with a 129-channel Biosemi system, pre-amplified sensors, and a DC coupling Amplifier, 24-bit A/D converter, 0.7 μV RMS/1.4 μV pp noise. Data that were outside a 0.1 Hz to 100 Hz frequency band were filtered out during the recording. Later, the data were further filtered using a band-pass digital filter with a range of 0.3 to 30 Hz to remove any unwanted frequency components. The reference was set to link mastoids. Two bipolar derivations were employed to monitor vertical and horizontal ocular movement electro-oculogram. Epochs were selected from continuous data, from -1.5 s to 1.5 s window around the offer and feedback releases. Eye movements or blink artifacts were corrected with independent component analysis, and remaining artifacts were rejected offline from trials that contained voltage fluctuations exceeding ± 200 μV, transients exceeding ± 100 μV, or

electro-oculogram activity exceeding ± 70 μV. EEG signal processing was implemented in MATLAB using in-house scripts (LAN toolbox, available online at http://lantoolbox.wikispaces.com/ (Zamorano *et al.*, 2014)).

1.6. EEG analysis

EEG signals were preprocessed using a 0.1-30 Hz band-pass filter. Eye blinks were identified by a threshold criterion of 100 μV, and their contribution was removed from each dataset using ICA. Other remaining artifacts (e.g., muscular artifacts) were detected using both an automatic artifact detection (voltage fluctuations exceeding ± 200 μV, transients exceeding ± 100 μV, electro-oculogram activity exceeding ± 70 μV and amplitude of frequency spectrum greater than 2 SDs in at least the 20% of the spectrum (0.3-30 Hz)) by visual inspection of the row signal and the spectrogram). All trials with remaining artifacts were rejected offline. All artifact-free trials were re-referenced to the all-electrode mean. Induced power distribution was computed using wavelets transform, with a seven-cycle Morlet wavelet, in -1.5 to 1.5-s windows around the offer (Billeke *et al.*, 2015). We displayed the result only for -1 to 1 s over the segmented signals to avoid edged artifact. For all analyses, we used the decibel of power related to the fixation phase as baseline (at the beginning of each game).

We calculated the models for each subject based on single trials (first-level analysis). Then, we computed a model for the decision phases (-1 to 1 second around the offer release).

For the decision/anticipatory phase, the model is as follows:

$$Power(f,t) = b1 + b2\ Risk(Logit)$$

where b1 is the intercept and b2 is the slope or coefficient for the variable Risk (Logit of the probability of acceptance of the offer, continuous variable given by the simulation). Then, we used the *t*-value of the model (time-frequency chart of *t*-values) of each subject as the input for the second level analysis.

This procedure presents a series of advantages over the classic categorical analysis. First, we used the *t*-value, which represents the mean normalized by the standard error. Then, we included the inter-individual variation in the analysis, thus improving the statistical inferences. Note that the classical categorical analysis uses only the mean, which is more sensitive to outliers and noise. Second, we avoided arbitrary classification (threshold) to separate riskier from safer offers. Finally, this analysis is less noisy and less sensitive to other artifacts. For further explicative examples, see the results of the Supplementary material of (Billeke *et al.*, 2015), where we compared this correlation analysis against a categorical analysis.

1.7. Source estimation

We defined 3x5005 sources constrained to the segmented cortical surface (three orthogonal sources at each spatial location), and computed a three-layer (scalp, inner skull, outer skull) boundary element conductivity model and the physical forward model (Clerc *et al.*, 2010). The measured electrode level data $X(t) = [x_1(t), \ldots, x_{n\_electrode}(t)]$ is assumed to be linearly related to a set of cortical sources $Y(t) = [y_1(t), \ldots, y_{n\_source}(t)]$ and additive noise $N(t)$: $X(t) = LY(t) + N(t)$, where L is the forward model. The inverse solution was then derived as $Y(t) = WX(t) = RL^T (LRL^T + \lambda^2 C)^{-1} X(t)$, where W is the inverse operator, R and C are the source and noise covariances respectively, the superscript T indicates the matrix transpose, and λ^2 is the regularization parameter. R was the identity matrix that was modified to implement depth-weighing (weighing exponent: 0.8 (Lin *et al.*, 2006)). The regularization parameter λ was set to 1/3. To estimate cortical activity at the cortical sources, the recorded raw EEG time series at the sensors x(t) were multiplied by the inverse operator W to yield the estimated source current, as a function of time, at the cortical surface: $Y(t) \sim WX(t)$. Since this is a linear transformation, it does not modify the spectral content of the underlying sources. It is therefore possible to undertake time-frequency analysis on the source space directly. For the physical forward model we used the individual anatomy. For each subject, four surfers (cortical surfer, inner skull, outer skull and scalp) were calculated. Then, the result of each cortical surface was normalized to a

standard default anatomy surface (Colin 27 from McConnell Brain Imaging Centre, Montreal Neurological Institute, McGill University, Montreal, Quebec).

To minimize the possibility of erroneous results we only present source estimations if there are both statistically significant differences at the electrode level and the differences at the source levels survive a multiple comparison correction. For these procedures we used MATLAB (LAN toolbox (Billeke *et al.*, 2013), available at http://lantoolbox.wikispaces.com/, BrainStorm (Tadel *et al.*, 2011) and open MEEG toolboxes (Gramfort *et al.*, 2011) and Freesurfer (Reuter *et al.*, 2012).

1.8. Functional imaging and analysis of brain connectivity

Images were slice-time corrected, realigned to the middle slice of the volume, normalized to the SPM8 default EPI template, and smoothed 4-mm FWHM Gaussian kernel. They were subsequently band-pass filtered (0.01-0.08 Hz). We finally regressed out the 6 motion parameters estimated during realignment.

2. Results

2.1. Demographic and neuropsychological results

No differences among groups were observed in age [$F(3, 81) = 2.49$, $P > .05$], education [$F(3, 81) = 1.14$, $P > .05$], gender [$x^2 = 7.61$, $df = 3$, $P > .05$], and handness [$F(3, 66) = 1.10$, $P > .05$). We observed an effect of basic cognitive screening (ACE-III) [$F(3, 80) = 18.11$, $P < .01$]. A post-hoc analysis (Tukey-s HSD, $MS = 113.37$, $df = 80$) revealed that controls outperformed bvFTD ($P < .01$) and AD ($P < .01$) patients. No differences were found between controls and FL. Significant differences were found in IFS total score [$F(3, 79) = 15.36$, $P < .01$] between patients and controls. A post-hoc analysis (Tukey-s HSD, $MS = 22.85$, $df = 79$) revealed that bvFTD ($P < .01$), AD ($P < .01$), and FL ($P < .05$) patients obtained an inferior performance than controls.

		bvFTD	AD	FL	CG	bvFTD vs CG	AD vs CG	FL vs CG
		N = 26	*N* = 21	*N* = 16	*N* = 22	*P* value	*P* value	*p* value
Demographic Variables	Age (years)	67.96 (11.42)	71.95 (6.37)	64.68 (5.92)	68.31 (5.80)	*N.S*	*N.S*	*N.S*
	Education (years)	13.92 (5.48)	12.52 (5.69)	13.06 (3.69)	15.09 (3.53)	*N.S*	*N.S*	*N.S*
	Gender (F:M)	12:14	16:5	7:9	16:6	*N.S*	*N.S*	*N.S*
europsychological Variables	ACE-III	73.57 (14.31)	70.76 (11.40)	84.43 (6.24)	91.95 (6.17)	< .01	< .01	*N.S*
	IFS	16.14 (6.72)	17.02 (4.39)	20.40 (4.13)	24.97 (1.95)	< .01	< .01	< .05

2.2 Acceptance Rate

We explored the acceptance rate and found no differences between groups (Kruskal-Wallis test, x^2 = 3.8, *P* = .2; means: controls = .54; bvDFT = .50; AD = .43, FL = .54). This finding is consistent with previous results obtained from other neuropsychiatric patients (Billeke et al., 2015).

2.3. Results from non-specific bargaining indexes

NRA index: We explored the first offer per game and found significant differences among groups (KW chi-squared = 12.17, *df* = 3, *P* < .01, Fig. 1s.a). Post-hoc analysis revealed that AD group tended to make lower offer in the first round of each game when compared with controls (*P* = .04), FL (*P* = .028), and bvFTD (*P* = .015).

CO index: The standard deviation of the offer throughout the rounds of each game was computed to estimate the consistency of social behaviors across the game. Fig.1s.b shows that significant differences were found among groups (KW chi-squared = 19.03, *df* = 3, *P* < .01). A post-hoc analysis revealed that control subjects were different from bvFTD (*P* < .01) and AD (*P* < .01). No differences were found between FL and controls.

2.4. Association between IFS and bargaining indexes

We found no association between the IFS total score and ASP index (Spearman's rank correlation r = .15, P > .05, all groups; bvFTD: r = .38, P = .08; AD r = -.009, P = .9; FL r = -.34, p = .21). Moreover, any significant correlation was observed between IFS total score and AOP index (Spearman's rank correlation r =- .10, P > .05, all groups; bvFTD: r = -.40, P = .07; AD: r = .16, P = .47; FL: r = .42, P = .11). Finally, no groups exhibited significant correlations between IFS total score and the SOIS index (Spearman's rank correlation r = .18, P > .05, all groups; bvFTD: r = .22, P = .33; AD: r = -.003, P = .9; FL: r = .25, P = .36).

2.5. *Association between bargaining indexes*

In order to investigate (i) the relationship between short-term and long- term decision making, (ii) and which factor contributed to the SOIS score, we calculated the association between the latter and both ASP and AOP. No correlation was found between AOP and SOIS (All groups: rho=0.02, P=.8; bvFTD: rho=0.06, P =.7; AD: rho=-0.04, P =.8; FL: rho=0.07, P =.7) or between ASP and SOIS (All groups: rho=0.12, P =.27; bvFTD: rho=0.20, P =.36; AD: rho=0.35, P =.11; FL: rho=-0.2, P =.38).

Moreover, we explored which factor can influence SOIS score by calculating the association between this and no-specific bargaining measure (CO, mean of the offer) and we did not find any correlation between SOIS and the mean of the offer (All groups: rho=-0.05, P =.6; bvDFT: rho=-0.12, P =.5; AD: rho=-0.35, P =.12; FL: rho=0.12, P =.66), or between CO and SOIS (All groups: rho=-0.06, P =.5; bvFTD: rho=0.10; P =.62; AD: rho=-0.34, P =.12; FL: rho=0.44, P =.08).

2.6. Oscillatory correlates of social bargaining

When we analyzed each patient group separately, we found that bvDFT did not present any modulation in the right temporo-pariental region, with significant differences with the control group in this region and in the medial frontal region (Wilcoxon test, and cluster

bases permutation test, cluster $P < .001$). The AD group presented an early modulation in temporo-pariental regions that did not differ from controls (Wilcoxon test, and cluster bases permutation test, cluster $P = .07$). Only in a late time window (700-900 ms), AD patients presented less modulation mainly in right temporo-parietal regions (Wilcoxon test, and cluster bases permutation test, cluster $P = .002$). Note that the early modulation of AD patients did not differs to of control group (Wilcoxon test $P > .05$ uncorrected). Finally, FL presented less modulation mainly in frontal electrodes, but they exhibited a difference in left temporo-parietal regions, where patients showed greater risk modulation relative to controls (Wilcoxon test, and cluster bases permutation test, cluster $P = .01$). However, note that due to the moderate number of participants, no major conclusion can be derived from each patient group results separately.

2.7. Functional connectivity

The analysis of the network estimated from controls subjects revealed a similar fronto-temporo-parietal distribution observed in the original (network estimated from all subjects (Fig.4S, A). Long-range connections were larger in controls and AD, but they were disrupted in bvFTD and FL (see Supplementary Fig. 4S, B and Table 7). Importantly, the spatial organization of the mid- and long-range connections was similar when we compared the groups exhibiting good (controls, AD) and bad (bvFTD, FL) performance using both the network estimated from all subjects and the network estimated from controls only (see Supplementary Fig.5S). Thus, the network estimated from controls resembled that estimated from all subjects, suggesting that the preserved performance of controls and AD depend on mid- and long-range connections of fronto-temporo-parietal networks.

3. Discussion

3.1. Behavioral Results

Some participants that expect their partner to change his/her acceptance threshold tend to maintain a relatively fixed behavior throughout the round of a game (Billeke *et al.*, 2014). This kind of behavior is also characterized by normal o lower variation of the offer. An extreme version of this behavior emerged in FLs patients. They presented lower SOIS scores and lower variation of the offer throughout the game (see CO results in the

Supplementary Material and Methods, section 2.3), thus suggesting an inflexible behavior which aligns with classical descriptions of frontal symptoms (Glascher *et al.*, 2012).

Another behavior related to SOIS score involves dwelling on the "negotiation" phase without reaching an agreement with a partner. This kind of behavior is characterized by lower SOIS values but normal or greater variation of the offer throughout a game, as observed in bvFTD (both lower SOIS and greater variation of the offers [see CO results in Supplementary Materials and Methods, section 2.3]). However, note that change in the variation of the offer is not necessarily correlated with lower SOIS scores. Indeed, previous findings indicate that schizophrenic patients have greater SOIS values than controls, together with greater variation in their offer (Billeke *et al.*, 2015).

Additionally, SOIS values could also reflect extremely inconsistent offers. However, we ruled out this possibility as all groups presented normal basic bargaining performance (ASP, OSP), and these parameters did not correlate with SOIS scores (Supplementary Results, section 2.5).

Interestingly, this distinction between behavioral patterns leading to lower SOIS scores aligns with findings at a neuroanatomical level. In the patient groups with greater variation in their offers (bvFTD and AD), SOIS correlated mainly with atrophy in the ventromedial prefrontal cortex, an area implicated in the integration of self- and other-preferences during social decision-making (Hutcherson *et al.*, 2015). In turn, the performance of FL patients exhibiting lower variation across offers (an inflexible behavior) was associated with right dorsolateral prefrontal structures. Interestingly, this region plays a role in strategic and norm-guided behavior, probably influencing social decision-making via modulations of ventromedial prefrontal cortex activity (Baumgartner *et al.*, 2011).

Finally, it is conceivable that SOIS variation reflects differences across the patients' risk-taking behavior. However, the mean of the patients' offer did not correlate with this measure (Supplementary Results, section 2.5). Indeed, AD patients made significantly lower offers relative to controls (Supplementary Results, section 2.3), but their SOIS indexes were normal. Thus, the offer may represent how subjects internalized the social norm of fairness (or, alternatively, a simple risk estimation), while SOIS represents a more

flexible parameter indicating how subjects integrate other- and self-perspectives in a long-term strategy aimed to reaching an agreement with their partners.

Supplementary Figures

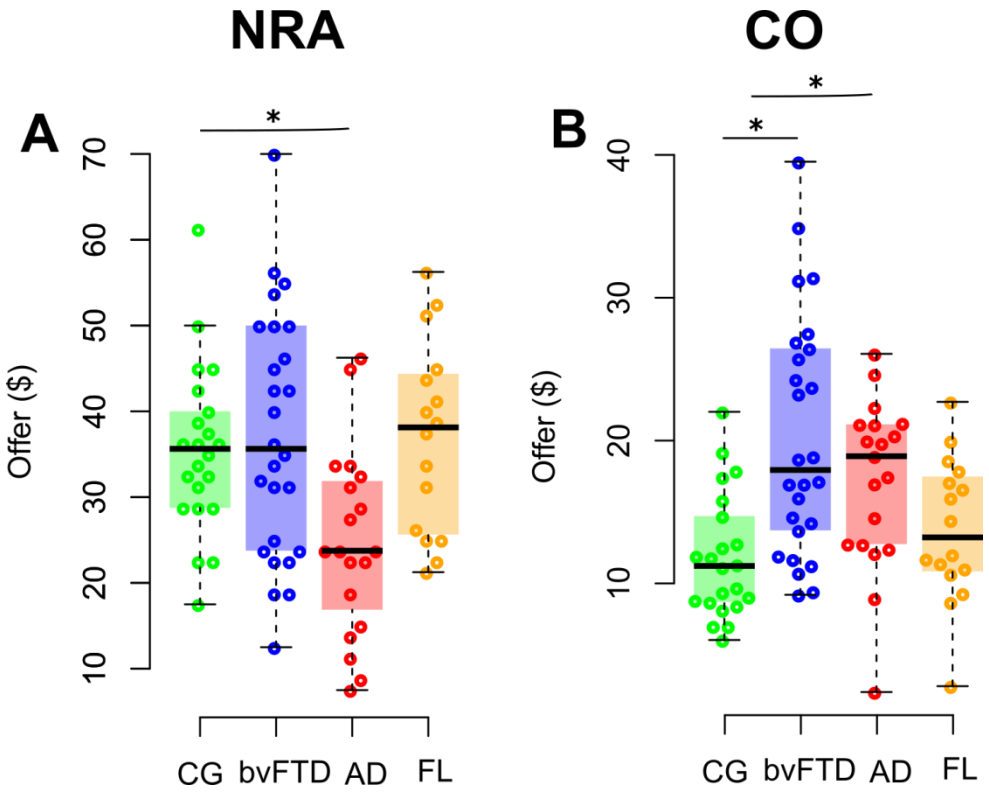

Figure 1S: Non-specific bargaining indexes. A: Offering behavior related to the first offer per subject in each game (NRA). Significant differences between controls and AD. B: Mean of the standard deviation of the offer through each game separated by group (CO). Significant differences between controls and bvFTD and between controls and AD. Circles represent subjects, broken lines represent the medians, and rectangles represent the interquartile segment. Green represents the healthy controls, blue represents patients with bvFTD, red represents patients with AD, and orange represents FL patients. *$p < .05$ (Intra-group analyses were performed with Wilcoxon's signed rank test; comparisons among groups were calculated with Kruskal-Wallis test, post hoc analysis were conducted with Dunn's test.) *NRA* = Normative risk adjustment; *CO* = Consistency of the offer; CG =

control group; bvFTD = behavioral variant of frontotemporal dementia; AD = Alzheimer disease; FL = frontal lesion.

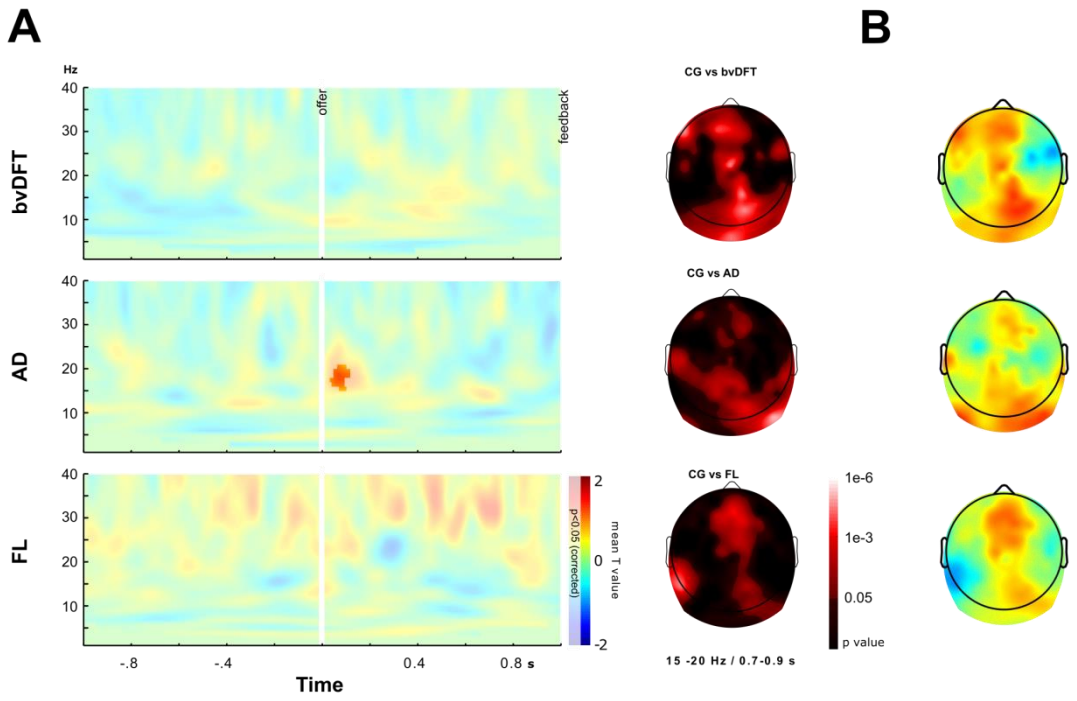

Figure 2S: Oscillatory correlates of social bargaining in each group. A: Time-frequency chart of the difference between bvFTD-CG, AD-CG, and FL-CG during the UG. Colors represent the mean across subjects of the *t* value of the individual correlation between the power of the oscillatory brain activity and the risk of the offer made. The clusters of significant effects are highlighted ($p < .01$ cluster-corrected). B: Topographic distribution and source estimation of significant cluster of apha/beta activity after the offer (15-20 Hz, 0.7-0.9 s) in the difference bvFTD-controls, AD-controls, and FL-controls. CG = control group; bvFTD = behavioral variant of frontotemporal dementia; AD = Alzheimer's disease; FL = frontal lesion

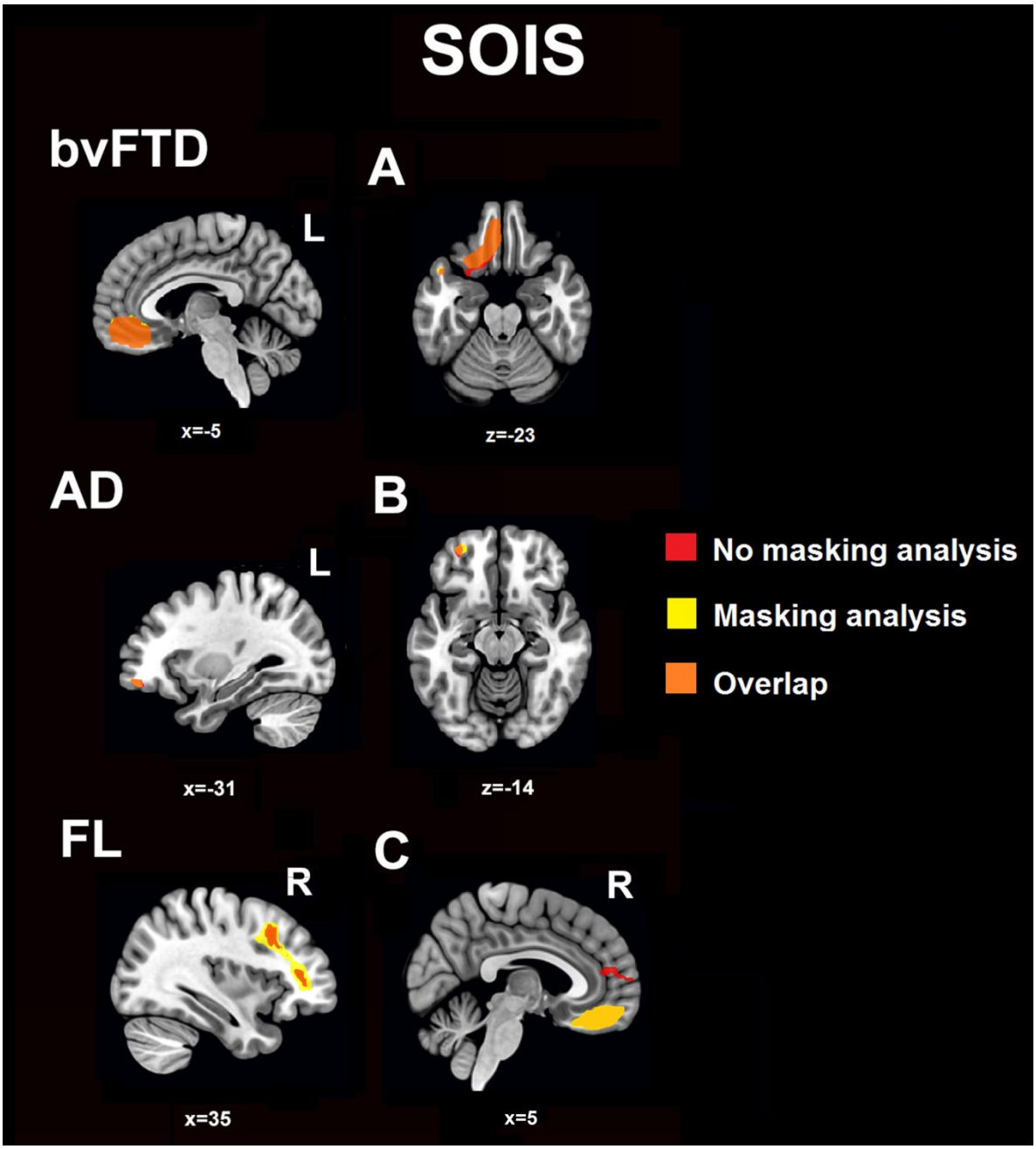

Figure 3S: Convergence of brain correlates of social bargaining using whole-brain analysis and masking. The regions that correlate with SOIS scores for each group are shown in red. The regions included in masking analysis that showed significant relations between SOIS scores and grey matter volume in each group are showed in yellow ($P < .05$, FDR corrected). bvFTD = behavioral variant of frontotemporal dementia; AD = Alzheimer's disease; FL = frontal lesion

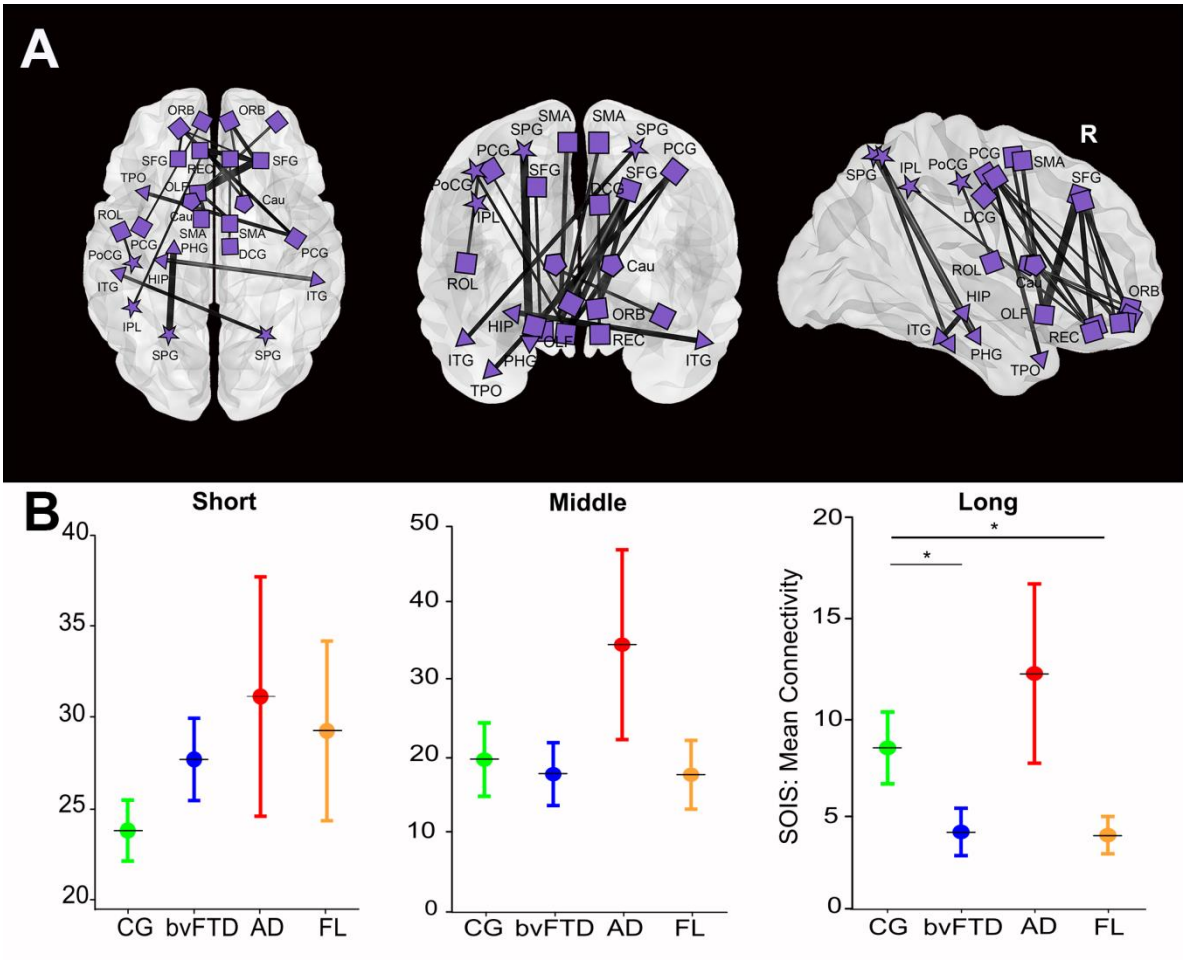

Figure 4S: SOIS-Functional connectivity association. *A*: Distributed network encompassing fronto-parieto-temporal connections showed by the association between functional connectivity and SOIS scores estimated from controls' networks. *B*: Different patterns of local-to-global connections in each group revealed by the analysis of the spatial distribution of nodes in this network. Reduced connections at medium- and long-range distances were observed in bvFTD and FL patients compared to controls. No differences between bvFTD and FL were observed. Significant results were obtained with a Monte Carlo permutation test combined with bootstrapping (P< 0.01). Cau = caudate; PHG = Parahippocampal gyrus; IPL = inferior parietal lobe; ITG = inferior temporal gyrus; ORB = orbitofrontal gyrus; OLF = olfactory gyrus; TPO = middle temporal pole; PoCG = postcentral gyrus; Rec = gyrus rectus; SFG = superior frontal gyrus; SPG = superior parietal gyrus; SMA = superior motor area; ROL = rolandic operculum. Abbreviations: CG

= controls; bvFTD = behavioral variant of frontotemporal dementia; AD = Alzheimer's disease; FL = frontal lesion.

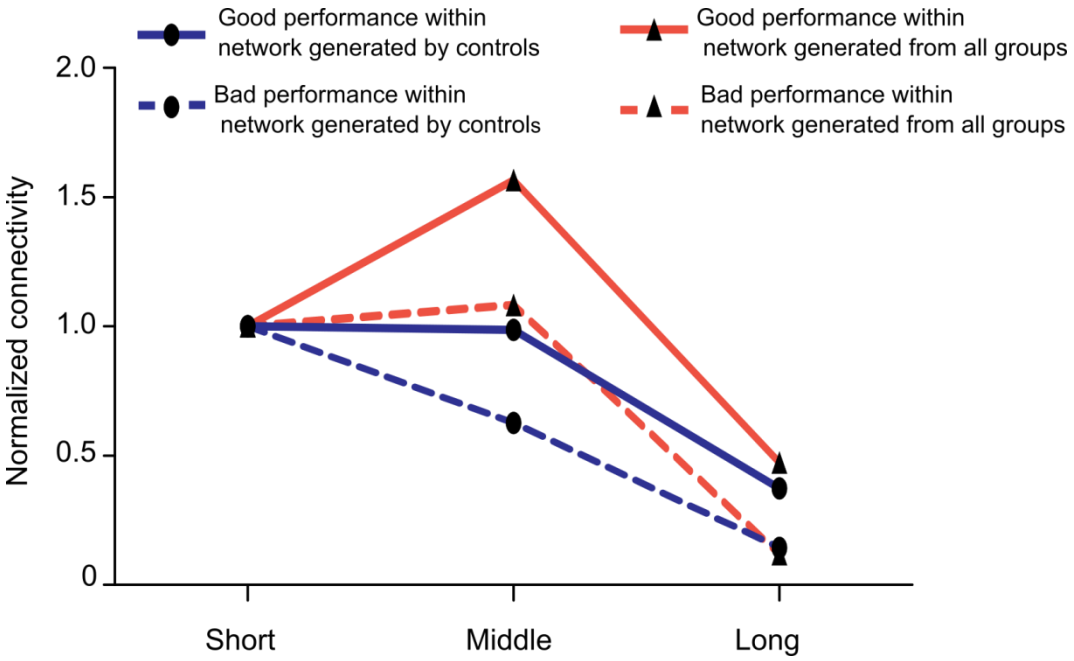

Figure 5S. Functional networks associated with SOIS's good vs. bad performance. Comparison of SOIS networks obtained from all groups (red) and from controls only (blue). Connectivity values are normalized (to the mean of short distance connectivity) for each comparison in each network. In both networks, the group with good performance (controls, AD) presented greater connectivity than the group with bad performance (bvFTD, FL) in mid- and long-range connections. Network estimated from controls subjects: Short-range connections: t = 0.460, P = -.75; Mid-range connections: t = 4.428, P = 1.9996e-04; Long-range connections: t = 9.282, P = 1.9996e-04. Network estimated from all subjects: Short-range connections: t = 1.693, P = .99; Mid-range connections: t = 6.970, P = 1.9996e-04; Long-range connections: t = 8.959, P = 1.9996e-04).

Supplementary Table 1: Clusters of significant grey matter reduction of bvFTD

Region	Cluster *k*	*x*	*y*	*z*	Peak *t*	Peak z
Left superior frontal gyrus	2559	-28	52	-1	6.3	5.18
Left superior orbito-frontal		-16	52	-12	5.46	4.66

cortex						
Left superior frontal gyrus		-15	52	-3	5.16	4.46
Left inferior frontal gyrus (orbitofrontalcortex)	508	-39	24	-9	4.15	3.74
Left inferior frontal gyrus (pars triangularis)	127	-39	42	6	3.99	3.63
Leftmiddle temporal gyrus	89	-45	9	-31	3.61	3.32

Supplementary Table 2: Clusters of significant grey matter reduction of AD

Region	**Cluster *k***	***x***	***y***	***z***	**Peak *t***	**Peak z**
Right parahippocampal gyrus	17157	29	-2	-34	5.47	4.44
Rightfusiform		41	-16	-27	4.62	3.93
Right inferior temporal gyrus		48	-10	-27	4.22	3.66
Left insula	16725	-39	-2	11	5.12	4.24
Left rolandic operculum		-47	-7	11	4.47	3.83
Left insula		-40	-1	-7	4.35	3.75
Left inferior temporal gyrus	2683	-51	-17	-27	4.41	3.79
Right olfactory (anterior cingulate)	2290	4	12	-10	4.36	3.76
Right inferior temporal gyrus	1683	42	-71	-9	4.2	3.65
Left superior temporal gyrus	3101	-59	-18	-3	4.18	3.63
Right posterior cingulate	6598	3	-48	26	4.11	3.59
Right precuneus		3	-55	22	4.09	3.57
Left posterior cingulate	2167	-6	-52	28	3.99	3.51
Left parahippocampus	2784	-25	-4	-30	3.96	3.49

Left hippocampus		-25	-8	-23	3.76	3.34
Right insula	2209	41	-2	13	3.93	3.46
Left amygdala	1249	-18	0	-16	3.89	3.44
Left middle frontal gyrus	522	-45	9	33	3.8	3.37
Left inferior occipital gyrus	289	-33	-81	-13	3.69	3.29
Left middle temporal gyrus	345	-57	-52	4	3.64	3.26
Left middle temporal gyrus	327	-62	-33	-2	3.62	3.24
Left hippocampus	684	-29	-24	-16	3.61	3.23
Right superior temporal gyrus	1023	48	-12	-8	3.57	3.2

Supplementary Table 3: Significant clusters associating behavioral scores to grey matter volumes of bvFTD and AD

Group	Region	Cluster *k*	*x*	*y*	*z*	Peak *t*	Peak z
BvFTD							
	Middle orbitofrontal gyrus	1854	-34	48	-10	13.25	> 8
	Rectus gyrus		-6	48	-20	12.05	7.63
	Inferior orbitofrontal gyrus		-38	36	-8	11.81	7.56
	Superior temporal gyrus	530	-40	16	-34	10.7	7.18
	Fusiform gyrus		-26	4	-42	8.08	6.1

	Inferior temporal gyrus		-34	0	-46	7.93	6.02
AD							
	Middle orbitofrontal gyrus	50	-32	52	-12	3.43	3.14

Supplementary Table 4: Motion parameters results

	CG	bvFTD	AD	FL	All groups	All groups
	Mean (SD)	*Mean (SD)*	*Mean (SD)*	*Mean (SD)*	*F*	*P value*
Mean translational (mm)	0.62 (0.40)	0.72 (0.62)	0.71 (0.48)	0.68 (0.30)	0.65	.584
Mean rotational (°)	0.53 (0.35)	0.92 (0.82)	0.99 (1.37)	0.83 (0.60)	0.17	.919

CG, bvFTD, AD, and FL values are provided in means (SD).

Supplementary Table 5: Range distance and number of links included into each range

	Range distance (mm)	CG	bvFTD	AD	FL
Long	94.09-141.14	10	4	3	17
Middle	47.05-94.09	38	25	23	33
Short	0-47.05	18	17	18	18

Supplementary Table 6: Results of the correlation between functional connectivity and SOIS index

		P (fdr)	R
Left tectus	Right superior temporal lobe	0.000	0.484
Right middle occipital	Right inferior occipital	0.000	0.430
Left superior parietal	Left middle temporal	0.000	0.422
Right superior parietal	Right middle temporal	0.001	0.412
Right superior occipital	Right middle temporal	0.001	0.409
Left parahippocampal	Left superior parietal	0.001	0.390
Right lingual	Right middle occipital	0.002	0.381
Left superior occipital	Right middle occipital	0.002	0.378
Right superior frontal	Right postcentral	0.002	0.374
Left cuneus	Right middle occipital	0.003	0.370
Right superior/ middle frontal	Right superior parietal	0.003	0.368
Left superior parietal	Right superior parietal	0.003	0.365

Supplementary Table 7: Differences in the spatial range of connections between controls and each clinical group

	CG vs bvFTD		CG vs AD		CG vs FL	
	T	*P value*	*T*	*P value*	*T*	*P value*
Short	-2.913	0.007	-4.227	1.9996e-04	-3.644	1.9996e-04
Middle	1.318	0.189	-4.809	1.9996e-04	1.232	0.234
Long	8.577	1.9996e-04	-3.276	0.001	9.137	1.9996e-04

Abbreviations: CG = controls; bvFTD = behavioral variant of frontotemporal dementia; AD = Alzheimer's disease; FL = frontal lesion. Significant results were obtained with a Monte Carlo permutation test combined with bootstrapping. Significant differences between each group and controls revealed hyperconnectivity in short connections (FL = AD = bvFTD > Controls). Mid- and long-range connections revealed hypoconnectivity in bvFTD and FL relative to controls.

REFERENCES

Baez S, Couto B, Torralva T, Sposato LA, Huepe D, Montanes P*, et al.* Comparing moral judgments of patients with frontotemporal dementia and frontal stroke. JAMA Neurol. 2014; 71(9): 1172-6.

Baumgartner T, Knoch D, Hotz P, Eisenegger C, Fehr E. Dorsolateral and ventromedial prefrontal cortex orchestrate normative choice. Nat Neurosci. 2011; 14(11): 1468-74.

Billeke P, Armijo A, Castillo D, Lopez T, Zamorano F, Cosmelli D*, et al.* Paradoxical Expectation: Oscillatory Brain Activity Reveals Social Interaction Impairment in Schizophrenia. Biol Psychiatry. 2015; 78(6): 421-31.

Billeke P, Zamorano F, Cosmelli D, Aboitiz F. Oscillatory brain activity correlates with risk perception and predicts social decisions. Cereb Cortex. 2013; 23(12): 2872-83.

Billeke P, Zamorano F, Lopez T, Rodriguez C, Cosmelli D, Aboitiz F. Someone has to give in: theta oscillations correlate with adaptive behavior in social bargaining. Soc Cogn Affect Neurosci. 2014; 9(12): 2041-8.

Clerc M, Gramfort A, Olivi E, Papadopoulo T. The symmetric BEM: bringing in more variables for better accuracy. In: Selma Supek AS, editor. 17th International Conference on Biomagnetism Advances in Biomagnetism – Biomag2010. Dubrovnik (Croatia): Springer Berlin Heidelberg; 2010. p. 109-12.
Garcia-Cordero I, Sedeno L, Fraiman D, Craiem D, de la Fuente LA, Salamone P*, et al.* Stroke and Neurodegeneration Induce Different Connectivity Aberrations in the Insula. Stroke. 2015; 46(9): 2673-7.
Glascher J, Adolphs R, Damasio H, Bechara A, Rudrauf D, Calamia M*, et al.* Lesion mapping of cognitive control and value-based decision making in the prefrontal cortex. Proc Natl Acad Sci U S A. 2012; 109(36): 14681-6.
Gleichgerrcht E, Torralva T, Roca M, Pose M, Manes F. The role of social cognition in moral judgment in frontotemporal dementia. Soc Neurosci. 2011; 6(2): 113-22.
Gramfort A, Papadopoulo T, Olivi E, Clerc M. Forward field computation with OpenMEEG. Comput Intell Neurosci. 2011; 2011: 923703.
Hutcherson CA, Bushong B, Rangel A. A Neurocomputational Model of Altruistic Choice and Its Implications. Neuron. 2015; 87(2): 451-62.
Lin FH, Witzel T, Ahlfors SP, Stufflebeam SM, Belliveau JW, Hamalainen MS. Assessing and improving the spatial accuracy in MEG source localization by depth-weighted minimum-norm estimates. Neuroimage. 2006; 31(1): 160-71.
McKhann G, Drachman D, Folstein M, Katzman R, Price D, Stadlan EM. Clinical diagnosis of Alzheimer's disease: report of the NINCDS-ADRDA Work Group under the auspices of Department of Health and Human Services Task Force on Alzheimer's Disease. Neurology. 1984; 34(7): 939-44.
Rascovsky K, Hodges JR, Knopman D, Mendez MF, Kramer JH, Neuhaus J*, et al.* Sensitivity of revised diagnostic criteria for the behavioural variant of frontotemporal dementia. Brain. 2011; 134(Pt 9): 2456-77.
Reuter M, Schmansky NJ, Rosas HD, Fischl B. Within-subject template estimation for unbiased longitudinal image analysis. Neuroimage. 2012; 61(4): 1402-18.
Tadel F, Baillet S, Mosher JC, Pantazis D, Leahy RM. Brainstorm: a user-friendly application for MEG/EEG analysis. Comput Intell Neurosci. 2011; 2011: 879716.
Torralva T, Roca M, Gleichgerrcht E, Bekinschtein T, Manes F. A neuropsychological battery to detect specific executive and social cognitive impairments in early frontotemporal dementia. Brain. 2009a; 132(Pt 5): 1299-309.
Torralva T, Roca M, Gleichgerrcht E, Lopez P, Manes F. INECO Frontal Screening (IFS): a brief, sensitive, and specific tool to assess executive functions in dementia. J Int Neuropsychol Soc. 2009b; 15(5): 777-86.
Zamorano F, Billeke P, Hurtado JM, Lopez V, Carrasco X, Ossandon T*, et al.* Temporal constraints of behavioral inhibition: relevance of inter-stimulus interval in a Go-Nogo task. PLoS One. 2014; 9(1): e87232.